# A Requirement for p120-catenin in the metastasis of invasive ductal breast cancer

Kurley, Sarah J ; Tischler, Verena ; Bierie, Brian ; Novitskiy, Sergey V ; Noske, Aurelia ; Varga, Zsuzsanna ; Zürrer-Härdi, Ursina ; Brandt, Simone ; Carnahan, Robert H ; Cook, Rebecca S ; Muller, William J ; Richmond, Ann ; Reynolds, Albert B

Abstract: We have examined the effects of targeted p120 KO in a PyMT mouse model of invasive ductal (mammary) cancer (IDC). Mosaic p120 ablation had little effect on primary tumor growth but caused significant pro-metastatic alterations in the tumor microenvironment leading ultimately to a marked increase in the number and size of pulmonary metastases. Surprisingly, although early effects of p120-ablation included decreased cell-cell adhesion and increased invasiveness, cells lacking p120 were almost entirely unable to colonized distant metastatic sites in vivo. The relevance of this observation to human IDC was established by analysis of a large clinical dataset of 1126 IDCs. As reported by others, p120 downregulation in primary IDC predicted worse overall survival. However, as in the mice, distant metastases were almost invariably p120 positive, even in matched cases where the primary tumors were p120 negative. Collectively, our results demonstrate a strong positive role for p120 (and presumably E-cadherin) during metastatic colonization of distant sites. On the other hand, downregulation of p120 in the primary tumor enhanced metastatic dissemination indirectly via pro-metastatic conditioning of the tumor microenvironment.

DOI: https://doi.org/10.1242/jcs.250639

# A Requirement for p120-catenin in the Metastasis of Invasive Ductal Breast Cancer

Sarah J. Kurley[1], Verena Tischler[2], Brian Bierie[3], Sergey V. Novitskiy[1], Aurelia Noske[2], Zsuzsanna Varga[2], Ursina Zürrer-Härdi[2,] Simone Brandt[2], Robert H. Carnahan[7,4], Rebecca S. Cook[1], William J. Muller[5,6], Ann Richmond[1,4], Albert B. Reynolds[1,4]

1) Department of Cancer Biology, Vanderbilt University, Nashville, TN, USA

2) Institute of Surgical Pathology, University Hospital Zurich, Zurich, Switzerland

3) Whitehead Institute for Biomedical Research, Cambridge, MA, USA

4) Vanderbilt-Ingram Cancer Center, Nashville, TN, USA

5) Goodman Cancer Centre, Montreal, Quebec, Canada

6) Departments of Biochemistry and Medicine, McGill University, Montreal, Quebec, Canada

7) Department of Pediatrics, Vanderbilt University, Nashville, TN, USA

Corresponding Author:
Albert B. Reynolds
Vanderbilt University Medical Center
771 PRB, 2220 Pierce Ave, Nashville, TN 37232
Phone: 615-343-9532
Fax: 615-936-6399
E-mail: al.reynolds@vanderbilt.edu

**Key Words:** p120 catenin, breast metastasis, colonization

**Summary Statement:** A requirement for p120-catenin in the metastasis of invasive ductal breast cancer



**JCS Advance Online Article. Posted on 2 November 2020**

**Abbreviations:**

Apc: Adenomatous polyposis coli gene

CD45: Cluster of differentiation 45 antigen which is synonymous with leukocyte common antigen

CD11b: Cluster of differentiation 11beta which is synonymous with integrin subunit alpha-M

DCIS: Ductal carcinoma in situ

EIF4G: Eukaryotic initiation factor 4 gamma

EMT: epithelial to mesenchymal transition

F4/80: antigen encoded by the Adgre1 locus used as a monocyte-macrophage marker in mice

IDC: Invasive ductal carcinoma

IRES: Internal ribosome entry site

KO: Knock-out

LOH: Loss of heterozygosity

MET: mesenchymal to epithelial transition

MMTV: Mouse mammary tumor virus

P120: the Delta catennin protein encoded by the CTNND1 gene

PyMT: Polyoma Middle T antigen

Rho: Family of GTPases that belongs to the Ras superfamily of proteins, includes Rac1, Cdc42 and RhoA

RNA: Ribonucleic acid

ROCK1: Rho associated coiled-coil containing protein kinase 1

RNA: Ribonucleic acid

RT-qPCR: Real-time quantitative polymerase chain reaction

WT: Wild type

**ABSTRACT**

We have examined the effects of targeted p120 KO in a PyMT mouse model of invasive ductal (mammary) cancer (IDC). Mosaic p120 ablation had little effect on primary tumor growth but caused significant pro-metastatic alterations in the tumor microenvironment leading ultimately to a marked increase in the number and size of pulmonary metastases. Surprisingly, although early effects of p120-ablation included decreased cell-cell adhesion and increased invasiveness, cells lacking p120 were almost entirely unable to colonized distant metastatic sites in vivo. The relevance of this observation to human IDC was established by analysis of a large clinical dataset of 1126 IDCs. As reported by others, p120 downregulation in primary IDC predicted worse overall survival. However, as in the mice, distant metastases were almost invariably p120 positive, even in matched cases where the primary tumors were p120 negative. Collectively, our results demonstrate a strong positive role for p120 (and presumably E-cadherin) during metastatic colonization of distant sites. On the other hand, downregulation of p120 in the primary tumor enhanced metastatic dissemination indirectly via pro-metastatic conditioning of the tumor microenvironment.

## INTRODUCTION

Breast cancer is the second most common cause of cancer-related death in women. Although management of the disease has improved significantly over the last 10 years, metastasis remains a significant problem and the leading cause of mortality. Nonetheless, metastatic dissemination is a remarkably inefficient process(Valastyan and Weinberg 2011). To successfully colonize distant sites in the body, cells from the primary tumor must acquire *de novo* the ability to (i) invade locally, (ii) enter into circulation (intravasate), (iii) exit from circulation at a distant location (extravasate), and (iv) thereafter survive as micrometastatic colonies in an otherwise hostile environment. Disseminated micrometastases are clinically undetectable and can remain dormant for years (Valastyan and Weinberg 2011, Brabletz 2012). The final and rate-limiting step in the metastatic cascade, termed colonization, occurs when micrometastatic lesions emerge from dormancy to form clinically relevant macrometastatic tumors.

Though many factors underlying these events are not well understood (Kang and Pantel 2013) metastasis is frequently linked to genetic and/or epigenetic dysregulation of E-cadherin, the predominant cell-cell adhesion molecule in epithelial tissues and master organizer of the epithelial phenotype (Fan, Jin et al. 2019). As with other classical cadherins, its extracellular domains connect like cells via calcium-dependent homophilic interaction (Kim, Tai et al. 2011). Strong adhesion, however, is critically dependent on a group of cytoplasmic cadherin binding partners, namely α-, β- and p120-catenins, each of which also contributes indispensably to E-cadherin's role as a tumor suppressor (Jeanes, Gottardi et al. 2008, Schackmann, Tenhagen et al. 2013, Sun, Zhang et al. 2014). Notably, direct interaction of E-cadherin with p120 is required for E-cadherin stability and retention on the cell surface. In many cell types, cadherin adhesion is compromised or lost altogether upon removal of p120, as the remaining components of the complex are then internalized by endocytosis and degraded (Thoreson, Anastasiadis et al. 2000, Ozawa 2003, Wehrendt, Carmona et al. 2016).

Consistent with these observations, experiments in mice based on targeted p120 ablation in various epithelial tissues have revealed potentially causal links to cancer in the salivary gland (Davis and Reynolds 2006) esophagus (Stairs, Bayne et al. 2011), skin (Perez-Moreno, Song et al. 2008), pancreas (Hendley, Wang et al. 2016), intestine (Smalley-Freed, Efimov et al. 2011), and breast (Kurley, Bierie et al. 2012, Schackmann, Klarenbeek et al. 2013, El Sharouni, Postma et al. 2017). *In vivo* p120 KO phenotypes vary widely, however, depending on the organ (Perez-Moreno, Davis et al. 2006, Oas, Xiao et al. 2010, Smalley-Freed, Efimov et al. 2010), the degree of p120 depletion (Richert, Phadke et al. 2005) and the context under which p120 depletion occurs (Mastracci, Tjan et al. 2005, Macpherson, Hooper et al. 2007, Short, Kondo et al. 2017). During prostate maturation, for example, adhesion is largely unaffected by p120 KO despite near-complete loss of E-cadherin (Kurley, Bierie et al. 2012). The developing mammary gland, on the other hand, is essentially

disassembled, as epithelial adhesion is lost altogether (Kurley, Bierie et al. 2012). Interestingly, tumorigenic effects of p120 ablation in the skin (Perez-Moreno, Song et al. 2008) and the esophagus (Stairs, Bayne et al. 2011) were linked not to defective adhesion but rather a cell-autonomous inflammatory response (Perez-Moreno, Davis et al. 2006, Smalley-Freed, Efimov et al. 2010, Stairs, Bayne et al. 2011, Hu 2012). By contrast, in *Apc* mouse models of intestinal cancer, tumorigenesis was effectively blocked upon loss of both p120 alleles due to synthetic lethal interaction with the loss of *Apc* (Short, Kondo et al. 2017). Loss of just one *p120* allele, on the other hand, resulted in up to a 10-fold increase in tumor multiplicity (Short, Kondo et al. 2017). In mouse models of pancreatic cancer, monoallelic *p120* ablation was associated with metastasis to the liver while loss of both p120 alleles led to pulmonary metastases (Reichert, Bakir et al. 2018) revealing an unexpected dose-dependent effect of p120 downregulation on metastatic organotropism.

In breast cancer (BC), specific subtypes have been selectively linked to altered levels of p120 and/or E-cadherin. Inflammatory BC, for example, is associated with p120 upregulation by an EIF4G and IRES-mediated mechanism that leads to abnormally stable E-cadherin and the formation of highly metastatic tumor emboli (Silvera and Schneider 2009)(Silvera, Arju et al. 2009). In contrast, lobular BC is associated with complete loss of E-cadherin at a very early stage in its development (Berx, Cleton-Jansen et al. 1995) (Vos, Cleton-Jansen et al. 1997, Singhai, Patil et al. 2011), a phenotype largely recapitulated by E-cadherin ablation in p53 KO mice (Schackmann, Klarenbeek et al. 2013)(Derksen, Braumuller et al. 2011). With the loss of E-cadherin, p120 mis-localizes to the cytoplasm and metastases occur by a ROCK1-dependent mechanism (Schackmann, van Amersfoort et al. 2011). Interestingly, p120 ablation in the same p53 mutant mouse generates tumors that are E-cadherin-deficient and metastatic but do not recapitulate the lobular phenotype (Schackmann, Klarenbeek et al. 2013)(Hernandez-Martinez, Ramkumar et al. 2019). The effects of p120-ablation, therefore, are not necessarily the same as those caused by the loss of E-cadherin. Invasive ductal BC (IDC) is by far the most common BC subtype, accounting for ~80% of all human BC. Of note, p120 downregulation occurs in over 50% of IDC (Sarrio, Perez-Mies et al. 2004) and has been linked to poor prognosis (Nakopoulou, Gakiopoulou-Givalou et al. 2002, Talvinen, Tuikkala et al. 2010). Two small studies report regions of complete p120 loss in approximately 10% of ductal carcinomas (Dillon, D'Aquila et al. 1998, Nakopoulou, Gakiopoulou-Givalou et al. 2002). Nonetheless, p120's role in tumor progression and metastasis of IDC remains unclear.

Using MMTV-Cre; $p120^{f/f}$ mice, we showed previously that p120 is essential for mammary gland development. Spontaneous Cre-mediated p120 ablation at the onset of puberty (week 3) results in a pool of essentially non-adherent, E-cadherin-depleted cells that are lost altogether by week 6 (Kurley, 2012). In the present study, we crossed these mice onto an MMTV-PyMT background (i.e., MMTV-Cre; $p120^{f/f}$; MMTV-PyMT) to examine the effect of p120 ablation in the context of a well characterized p53-independent mouse model of invasive ductal mammary carcinoma (IDC). Oncogenic transformation by PyMT rescued the p120 null population, which in spite of near complete loss of E- and P-cadherins, was then efficiently retained as p120 null and/or mosaic p120+/- primary

tumors. The current study reports the outcome of these p120-ablation experiments on tumorigenesis and pulmonary metastasis.

## Results

### Characterization of p120 ablation in the *MMTV-PyMT* mouse model of breast cancer.

To examine the role of p120 in ductal breast cancer metastasis, we crossed our previously described mammary-specific p120 knockout mouse (*MMTV-Cre; p120*$^{fl/fl}$)(Perez-Moreno, Davis et al. 2006, Kurley, Bierie et al. 2012) to a well-characterized *MMTV-PyMT* mouse model of breast cancer (Lin, Jones et al. 2003). In the experimental cohort from this cross (*MMTV-Cre; p120*$^{fl/fl}$*; MMTV-PyMT*), PyMT expression and p120 ablation were induced simultaneously upon activation of the MMTV promoter at puberty (~3-4 weeks of age). We showed previously that in the absence of a transforming event, *MMTV*-Cre-induced p120 null cells were cleared from the developing gland and lost altogether by the end of week 6, after which the gland was reconstituted normally from p120-retaining stem cells (Kurley, Bierie et al. 2012). Here, we show that in the context of PyMT-induced transformation, p120-null cells are rescued and retained in primary tumors (Figure 1ABC). Depending on the animal, the overall proportion of tumor cells lacking p120 ranged from ~22 - 58% (38% average) (Figure 1B). p120 null regions of these primary tumors retained significant Keratin-8 positivity (Figure 1C), suggesting overall retention of epithelial identity. Surprisingly, mosaic p120 ablation did not affect primary tumor latency or primary tumor volume (Figure 1D, E), and differences in carcinoma cell apoptosis and proliferation were not statistically significant (Figure S1 A, B).

To assess the overall impact of p120 ablation on the E-cadherin complex, we immuno-labeled p120 positive and negative tumors with antibodies to E-cadherin and β-catenin (Figure S1C, D). p120 KO in the context of mT resulted in nearly complete loss of both E-cadherin and junctional β-catenin, as was previously observed in the absence of mT expression (Kurley, Bierie et al. 2012). Loss of the E-cadherin complex occurs to varying degrees upon p120 ablation as previously demonstrated in many epithelial tissues(Davis and Reynolds 2006, Perez-Moreno, Davis et al. 2006, Stairs, Bayne et al. 2011, Kurley, Bierie et al. 2012) but the mammary gland is unusual in that E-cadherin staining is almost abolished by p120 KO.

MMTV-PyMT tumors typically display a mix of distinct morphological features during progression. In the absence of p120, we observed that hyperplastic p120 negative lesions contained epithelial cells with a more rounded morphology and increased intraluminal sloughing (Figure S2A), apparently reflecting adhesion defects linked to E-cadherin loss. In addition, whereas late-stage MMTV-PyMT tumors typically contain a roughly even mix of pseudopapillary and characteristic adenocarcinoma phenotypes (Chetty and Serra 2008), their p120-null counterparts were almost exclusively pseudopapillary (Figure S2B).

**p120 ablation blocks pulmonary metastatic colonization**

To determine the effect of p120 on pulmonary metastasis, we examined whole mounts of lungs from control and p120 KO MMTV-PyMT animals that were collected 54 days following initial tumor palpation (Figure 2). Notably, metastatic lesions in the p120 KO model were substantially larger (Figure 2A; quantified in 2C) and four-fold more numerous (median of 3 in controls compared to 12.5 in KOs) (Fig. 2B) than those from p120 positive controls, revealing a strong, apparently pro-metastatic impact of p120 ablation. Surprisingly, however, immunolabelling experiments revealed that the actual pulmonary metastases from p120 KO animals were predominantly p120 positive (Figures 2D & 2E). Examples of the p120 content of individual pulmonary metastases from these animals are shown in figure 2D (i.e., positive, mixed, negative). To document the overall distribution of p120 positivity, metastases were scored as entirely positive, mostly positive, mostly negative, or entirely negative, and then quantified in each of six randomly selected p120 KO mice (Figure 2E).

Of note, entirely p120 negative metastases were exceedingly rare. They manifested in one animal only (mouse #6) and comprised only 15% of the total number of lung metastases in that animal (as opposed to 70% entirely positive). By contrast, in two animals (numbers 4 & 5), all of the metastases were entirely p120 positive. Moreover, irrespective of the mix, metastases in all six animals demonstrated strong selection for p120 positivity. These data suggest that despite the pro-metastatic effects of p120 ablation in primary tumors, retention of p120 confers a strong selective advantage with respect to establishing distant metastases.

To identify particular events in the process that might account for this enrichment, we used Cre recombinase-based methods to generate matched sets of polyclonal and monoclonal p120 positive (WT) and p120 negative (KO) PyMT tumor cell lines (Figure 3). As shown previously *in vivo* (Figures 1 and S1), p120 null cells displayed near absent levels of E-cadherin, but retained expression of the epithelial marker Keratin 8 (Figure 3A), suggesting retention of epithelial identity. Note that among the p120-null cell lines isolated from individual tumors, there were occasional p120 positive cells that served as internal positive controls (e.g., Fig. 3A, lower left panel). Interestingly, p120 KO induced superficial characteristics of mesenchymal cells (Figure 3A, bright field panels), raising the possibility a bone fide EMT. On the other hand, loss of intercellular adhesion following p120 ablation is expected to phenocopy many of the effects of EMT. Although not necessarily definitive, we observed that mRNAs typically upregulated by classical EMT (e.g., vimentin, snail, slug, Zeb1, SMA, S1004A) were not upregulated in a microarray dataset derived from p120 KO PyMT cells (data not shown). The simplest interpretation of these data, therefore, is that the mesenchymal-like phenotype observed is instead due to adhesive defects caused by p120 ablation.

*In vivo* effects of p120 ablation on tumor initiation and progression were assayed by transplanting isogenic p120 positive and negative PyMT cell lines into the cleared mammary fat pads of wild-type recipients. Similar to the results observed in the autochthonous mouse models, primary tumor latency and growth were not significantly affected by the absence of p120 (Fig. 3B). However, lung

metastases were evident in 77.8% of mice transplanted with p120 positive tumor cells, whereas metastases were virtually absent from mice transplanted with the isogenic p120-null counterparts (Fig. 3C). Thus, p120 KO in this model had relatively minor effects at the level of the primary tumor but almost completely blocked the formation of distant metastases.

To identify which stage(s) of the metastatic cascade were impaired by p120 loss, we assayed several metastasis-associated parameters, comparing MMTV-PyMT-transformed cell lines (controls) to their p120 KO counterparts. Cell motility was examined by an *in vitro* wound-healing assay. In the presence of p120, "wounded" cell monolayers were closed primarily by a process of collective migration. By contrast, p120 KO cells exhibited primarily single cell migration, which was only marginally less efficient (Kurley, Bierie et al. 2012)(Sup Vid). *In vitro* invasion assays, on the other hand, showed that p120 KO cells were 2 - 10 fold more efficient at penetrating transwell filters coated with matrigel, a model extracellular matrix (Figure 3D). Intravasation and survival in the bloodstream is typically assayed by quantification of circulating tumor cells in blood. However, for reasons that are unclear, the method is notoriously difficult to reproduce in MMTV-PyMT mouse models (Muraoka, Lenferink et al. 2002). Although we found no statistical difference in the results from control and p120-ablated animals, the number of cells isolated were typically low and highly variable in both cohorts (Supp. Fig. S3A and B). Taken together, however, these data suggest that p120-ablation enhances several mesenchymal cellular characteristics, including fibroblast-like morphology, a transition from collective- to single-cell migration, and a marked increase in invasive behavior, alterations likely to be pro-metastatic with respect to the early steps in the metastatic cascade.

As mentioned, generally acknowledged properties associated with metastatic capacity include the ability to (i) intravasate, (ii) survive in the bloodstream, (iii) extravasate, and/or (iv) survive and proliferate post-extravasation in effectively hostile foreign microenvironments. To further examine the ability of cells to survive in circulation and subsequently extravasate, isogenic p120 positive or negative PyMT tumor cells were labeled with a fluorescent dye and injected directly into circulation via the tail vein. Intraluminal survival/extravasation and subsequent clearance from the lungs were monitored by fluorescence microscopy at 1- and 6-hour time points, respectively (Supp. Fig. S3 C). p120 ablation, however, did not affect the number of cells retained in the lung at either time point, suggesting that p120 KO does not substantially alter the kinetics of extravasation and/or the subsequent clearance from the lung.

In the metastatic cascade, progression from disseminated micrometastases to clinically relevant macrometastatic lesions, is referred to as metastatic colonization. We postulated that p120 might be essential for (i) formation/survival of micrometastatic lesions, or alternatively, (ii) for the outgrowth of established micrometastases into macroscopic secondary tumors. To test the hypothesis, isogenic p120 positive or negative PyMT cell lines were tail vein injected and assayed 21 days later for metastatic colonization of the lung (Fig. 3F-H). Remarkably, WT PyMT-transformed cells (i.e., p120

positive) formed large numbers of macrometastatic lesions while their isogenic p120 KO counterparts were completely deficient in this process.

To clarify the underlying mechanism(s), we conducted soft agar colony formation assays to determine whether p120 KO cells were capable of anchorage-independent cell growth, an *in vitro* surrogate for tumorigenicity. We found that p120 ablation eliminated an otherwise robust ability of WT PyMT cells to undergo anchorage-independent cell growth. Thus, p120-loss in PyMT transformed cells confers a cell-intrinsic anchorage-independent growth defect that may be related to its *in vivo* defect in pulmonary colonization (Fig. 3E).

**p120-dependent regulation of the primary tumor microenvironment**

Paradoxically, although p120-ablation markedly increased the size and number of pulmonary metastases, the actual metastatic lesions were almost invariably p120 positive. A potential explanation is that the p120-ablated component of primary PyMT tumors might indirectly promote a significant pro-metastatic microenvironment. For example, p120 ablation in some tissues (e.g., skin, esophagus) leads to cell-autonomous inflammation that has been causally linked to tumorigenesis (Perez-Moreno, Song et al. 2008, Stairs, Bayne et al. 2011). Thus, we interrogated the primary tumor microenvironments from cohorts of PyMT and PyMT/p120 KO mice (Fig. 4). Notably, significantly increased abundance of macrophages (F4/80 positive) and myofibroblasts (SMA positive) were observed in regions of p120 ablation (Figures 4A and 4B, respectively). Trichrome blue staining indicated higher levels of collagen deposition in the p120-null tumors (Fig. 4C). Other cell populations within the primary tumor microenvironment, including several types of vasculature and CD3+ T-cells, were consistent between the two models (Figure S5 A-C). Overall, these data illustrate distinct alterations in the tumor stroma associated with p120-ablated epithelium.

To further characterize the primary tumor microenvironment, we analyzed macrophage infiltration and phenotype by flow cytometry and qRT-PCR. To quantify macrophage recruitment, tumors were dissociated and viable cells were analyzed by flow cytometry using antibodies that collectively detect macrophages (CD45+, CD11b+, F4/80+). By this method, total macrophage numbers were unaltered in PyMT p120 KO mice (data not shown). Thus, F4/80 positive macrophage populations observed in figure 2A may reflect locally enhanced recruitment to regions of p120 ablation, as opposed to the whole tumor. Macrophages exist in a variety of phenotypic states, including anti-tumor M1 and pro-tumor/pro-metastasis M2 (DeNardo and Coussens 2007). By flow cytometry using well-established M1 and M2 markers, the proportion of M1-like tumor macrophages were similar in p120 WT and p120 KO samples. However, M2 macrophages, were significantly increased in p120 knockout tumors (Figure 4D), suggesting a pro-tumor/pro-metastasis bias. To assess transcript levels, RNA from flow-sorted populations of CD45+CD11b+F4/80+ tumor macrophages was assessed by RT-qPCR analyses. Results from this analysis revealed significantly increased *Mmp2* and *Mmp9* (M2-like markers), and decreased M1-like markers *TNFα,* and *IL12β* (Figure 4E), confirming a shift in tumor macrophage phenotypes that is consistent with pro-metastatic

progression. Therefore, we postulated that p120-ablated tumor cells might selectively secrete factors known to function in the recruitment of macrophages. Conditioned media from p120-negative PyMT cells was 3- to 10-fold more effective in the *in vitro* recruitment of peritoneal macrophages than media from control (p120-positive) cells (Figure 4F). Thus, p120 ablation in the context of PyMT-expressing mammary tumor cells elicits secretion of as yet unidentified factors that may account for the activities of p120-negative PyMT cells in the recruitment and/or behavior of resident macrophage populations.

**Reduced p120 in primary tumors associates with a less-favorable outcome.**

p120 levels are frequently reduced and sometimes lost altogether in a wide variety of epithelial cancer types, including breast (Thoreson, Anastasiadis et al. 2000). To clarify inconsistencies in the pathology literature on ductal breast cancer, p120 expression was examined by immunohistochemistry in a cohort of 1126 patients with primary invasive ductal breast cancer. Details of the patient cohort are provided in Supplemental Table 1. Figure 5A shows representative examples of p120 expression in invasive ductal breast cancer corresponding to IHC scores 0 – 3 (panels i - iv), as compared to normal breast (panel v) and ductal carcinoma in situ (DCIS) stained for p63 (panel vi) or p120 (panel vii). High p120 expression (score 3) was observed in 49.7% of the primary tumor samples, similar to p120 staining intensity seen in normal breast (score 3) (Fig. 5A, Table 1). Complete loss of p120 (e.g., Fig.5A, panel *i*) was observed in 7.5% of the cases.

Partial p120 loss (scores 1 and 2) and complete 120 loss (score = 0) correlated with higher tumor grade, higher pT stage and estrogen receptor negativity (Table 1). We found no correlations with other parameters such as nodal stage and *HER2* status, and nearly all DCIS cases (128/129, 99.2%) showed strong (score = 3) p120 expression (e.g., Fig. 5A, panel iv,). Staining for p120 was localized primarily to plasma membranes, and cytoplasmic p120 expression was observed in only 96/1126 (8.5%), consistent with previously published data on ductal breast cancer (Sarrio, Perez-Mies et al. 2004).

Overall, statistical analyses show that reduced or absent p120 in primary invasive ductal breast cancer is significantly associated with worse outcome (Figure 5B). By multivariate analysis, p120 did not qualify as an independent prognostic factor (compared with pT, grade, pN, and with/without estrogen receptor). However, patients with complete or partial loss of membranous p120 expression had significantly shortened overall survival in a univariate analysis (*p=0.027*) (Figure 5B). Also, patients whose tumors showed complete p120 loss (score 0, n=73) versus all other levels (score 1-3, n=862) at the time of histology had a significantly shorter overall survival (p=0.011).

**p120 loss in distant and/or lymph node metastases is rare.**

Extending the analysis to breast cancer metastatic lesions, we initially examined p120 in 225 lymph node and 11 distant (non-lymph node) metastases. Immunohistochemistry for p120 in lymph node

metastases (n=225) indicated strong expression in 48.9% of cases (110/225) (score 3), reduced expression in 36.9% (83/225) (score 2), weak expression in 12.4% (28/225) (score 1), and absent p120 staining in 1.8% (4/225). In the set of distant (non-lymph node) metastases (n=11), p120 was expressed in 100% of cases (45.5% scored 1 or 2, 54.5% scored 3) (Fig. 5C).

Next, we interrogated a set of metastases from individuals whose primary tumors were p120 negative. Of the 84 primary invasive ductal breast cancer cases with complete loss of membranous p120 staining, 14 cases of matched metastatic disease (16.7%) were available from the archives. Of these, 5/14 (35.7%) expressed high levels of p120 (score 3), 5/14 (35.7%) showed reduced levels (score = 2), 3/14 (21.5%) scored weakly (score = 1) and one (7.1%) was negative (score = 0) (Figure 5D). Thus, despite complete absence of p120 staining in all 14 primary tumors, all but one of the metastases were p120 positive, and the majority (10/14) were either normal (5/14, score 3) or moderately reduced (5/14, score 2).

**Discussion**

The vast majority of human BC (~80%) manifests as IDC, as modeled here in MMTV-PYmT mice. Downregulation of p120 in IDC is associated with poor prognosis (Saijo, Sato et al. 2001, Wijnhoven, Pignatelli et al. 2005), but underlying mechanism(s) are not well understood. Importantly, we found that pulmonary metastases obtained from human IDC patients were almost invariably positive for p120, even in matched samples where the primary tumors were p120 negative. This seeming contradiction is addressed in the current study using mouse models for insight into mechanism and human IDC to validate our observations in mice.

We previously demonstrated that MMTV-targeted p120 ablation during development of the mammary gland resulted in completely non-adherent cells that were unable to participate in formation of the gland. By six weeks, this non-adherent pool was lost altogether and replaced by normal mammary tissue reconstituted from a residual pool of p120-retaining stem cells (Kurley, Bierie et al. 2012). In the current study, we used the MMTV-mT mouse model to directly examine the effects of mosaic p120 ablation in the context of a transforming oncogene. Indeed, transformation by PyMT rescued the viability of a p120-negative pool that otherwise did not survive. Unexpectedly, however, the absence of p120 did not exacerbate metastasis, but rather suppressed the strong metastatic proficiency normally conferred by PyMT.

Collectively, our results suggest a strong selective pressure for retention of p120 during metastatic colonization of distant sites. To validate this hypothesis experimentally, we generated isogenic mT-transformed cell lines differing only by the presence or absence of p120. Notably, in orthotopic implantation experiments, the absence of p120 had little impact on primary tumor latency or volume, as observed initially in the autochthonous model, but metastasis was abolished. This effect was particularly striking when assayed by tail vein injection (i.e., lung colonization assays), a procedure

that bypasses the primary tumor altogether to pinpoint activities that are selectively relevant to the colonization of distant sites. Remarkably, p120-ablated cell lines exhibited no evidence of colonization, whereas their p120 expressing parental counterparts were aggressively metastatic. Consistent with these data, p120-ablation also eliminated an otherwise robust ability of these cells to undergo anchorage-independent cell growth. Thus, expression of p120 in these mT-transformed cell lines is apparently required for anchorage-independent growth, and importantly, for distant metastatic colonization.

This requirement for p120 during metastatic colonization is most- likely explained by its essential role in maintaining E-cadherin stability. Despite E-cadherin's reputation as a potent metastasis suppressor, compelling evidence suggests that several modes of metastatic dissemination and or colonization may actually depend on the expression or re-expression of E-cadherin. In general, models to this effect fall into one of two main categories. The first invokes metastatic dissemination by collective migration (Huang, Jolly et al. 2015, VanderVorst, Dreyer et al. 2019) (Cheung and Ewald 2016), a process known to require p120 and its stabilizing effect on E-cadherin (Macpherson, Hooper et al. 2007, Kota, Terrell et al. 2019, Gritsenko, Atlasy et al. 2020). The second invokes dissemination via an epithelial to mesenchymal transition (EMT), which confers a spectrum of mesenchymal traits that enable and/or promote metastatic behavior (e.g., exchange of E-cadherin for N-cadherin, mesenchymal cell morphology, invasive behavior, cancer stem cell properties, anchorage-independence) (Jones, Wang et al. 2014, Hernandez-Martinez, Ramkumar et al. 2019). Importantly, EMT is reversible, and several lines of evidence suggest that successful metastatic colonization following dissemination by EMT depends ultimately on the reversal of this process (i.e., mesenchymal to epithelial transition / MET), as evidenced in part by frequent re-expression of E-cadherin in distant metastatic lesions (i.e., MET) (Wells, Yates et al. 2008, Brabletz 2012, Gunasinghe, Wells et al. 2012). A third model suggested recently by Ewald and colleagues poses an essential role for E-cadherin as a survival factor (Padmanaban et al., 2019). Absent E-cadherin, increased TGF□3 signaling leads to elevated levels of reactive oxygen species and an apoptotic response to conditions imposed by the metastatic cascade. Notably, all of these models ultimately posit essential roles for E-cadherin that are p120-dependent.

A hallmark of classic EMT (and partial manifestations thereof) is the upregulation of a mesenchymal cadherin (usually N-cadherin) at the expense of E-cadherin, whose expression is simultaneously reduced or lost altogether. The mesenchymal properties of N-cadherin are closely associated with increased cell motility, invasion, and other aspects of metastatic dissemination (Thiery, Boyer et al. 1988, Gritsenko, Atlasy et al. 2020). Like most, if not all, classical cadherins, however, the stability of N-cadherin is also p120-dependent. Thus, in the context of EMT-mediated metastatic dissemination, p120 ablation might conceivably impair early events in the metastatic cascade via destabilization of N-cadherin, and/or late events (e.g., MET, colonization), via destabilization of E-cadherin. Variations on this theme have been proposed for collective migration and the models are

not necessarily mutually exclusive (Thiery, Boyer et al. 1988, Wagner, Roderburg et al. 2007, Theveneau and Mayor 2012, Peglion, Llense et al. 2014).

These observations are important because dysregulation of E-cadherin function and/or expression to varying degrees is evident in the vast majority of human cancer, 90% of which is epithelial in origin. The effects are generally interpreted in the obvious context of adhesion. However, our findings suggest that p120 and/or E-cadherin dysfunction may have other important consequences, including pro-metastatic conditioning of the tumor microenvironment, that are not yet fully appreciated. Moreover, this is not the first report of significant adverse consequences to the microenvironment associated with conditional p120 ablation. Although effects vary widely, depending on the tissue, p120 ablation in the skin (Perez-Moreno, Davis et al. 2006) or the esophagus (Stairs, Bayne et al. 2011) have significant inflammatory effects that appear to be causally linked to tumorigenesis. The possibility that such effects contribute significantly to the immune and microenvironmental conditions underlying tumorigenesis remains largely unexplored.

Though paradoxical at face value, our data are consistent with the notion of distinct roles for p120 at different stages of the metastatic cascade. In the mouse model used herein (MMTV-mT; MMTV-Cre; $p120^{fl/fl}$), MMTV is activated around three weeks of age and controls both the tumor-initiating event (i.e, expression of mT) and the timing of p120 ablation (via upregulation of Cre), which occur more or less simultaneously. Thus, p120-ablation is, by definition, a very early event in this model that clearly increases both the number and size of p120-positive pulmonary metastatic lesions.

There are two general models relevant to the nature and timing of metastatic dissemination (Peglion, Llense et al. 2014, VanderVorst, Dreyer et al. 2019) (Huang, Jolly et al. 2015, Kota, Terrell et al. 2019). The "linear" progression model posits that metastasis-competent subclones arise late in tumor progression due to accumulation over time of genetic and epigenetic alterations. According to this model, metastases typically develop from aggressive late-stage subclones of the primary tumor and therefore share, at least initially, the same spectrum of genetic alterations. For example, if loss of p120 (or E-cadherin) were to trigger metastasis directly, one might expect this event to be reflected in the actual metastases, but that is not what we observed. p120 null cells were almost entirely excluded from metastatic lesions. This result is particularly striking in experiments where the early stages of metastasis are bypassed altogether by introducing the p120 null cells directly into the blood via tail vein injection.

In contrast, the "parallel" progression model suggests that metastatic dissemination is an early event and that primary and metastatic clones evolve independently thereafter. Loss of E-cadherin, for example, is typically viewed as a late event in tumor progression and a key mediator of the transition to metastasis. In our experiments, however, deletion of p120 was, by definition, an early event, and the metastatic lesions exacerbated by this event did not contain this mutation. Thus, we suggest that the early effects of p120 ablation with respect to successful metastatic colonization are not cell autonomous. Instead, the metastasis promoting effects of the p120 null cell pool appear to manifest

indirectly at the level of the primary tumor, most likely functioning to accelerate dissemination of p120 expressing cells. Thereafter, retention of p120 becomes a major discriminating factor with respect to successful metastatic colonization.

We showed recently in Adenomatous Polyposis Coli (Apc) mouse models of intestinal cancer that loss of one p120 allele dramatically increases tumor multiplicity. Surprisingly, however, loss of the second allele did not further enhance tumorigenesis, but rather turned out to be synthetic lethal with loss of Apc. Thus, complete loss of p120 was never observed in these Apc-LOH-initiated tumors because intestinal stem cells exhibiting loss of both proteins were rapidly eliminated (Short, Kondo et al. 2017, Short, Barrett et al. 2019). This phenomenon applies to α-catenin and E-cadherin as well, providing a compelling explanation for why complete loss of E-cadherin function is almost invariably a late event in intestinal cancer. These observations clearly imply the existence of a failsafe mechanism that somehow restricts complete loss of E-cadherin function during the early stages of intestinal tumor formation. Complete loss of E-cadherin function does, however, occur in late-stage tumors, suggesting that the failsafe mechanism(s) itself eventually fails as tumors progress to malignancy.

In closing, it is worth mentioning that retention of p120 (and E-cadherin) at distant metastatic sites was surprising, in part, because E-cadherin is widely viewed as a metastasis suppressor. By any conventional interpretation of the literature, one would expect metastases promoted by p120-ablation to be comprised largely, if not entirely, of p120-negative (E-cadherin-deficient) cells. Instead, our results reveal a strong selective pressure for p120 retention and are largely in line with a rapidly emerging literature on E-cadherin. In particular, it is increasingly clear that several modes of metastatic dissemination and/or colonization are dependent on the expression or re-expression of E-cadherin. One example is metastatic dissemination by collective migration (Huang, Jolly et al. 2015, VanderVorst, Dreyer et al. 2019) (Cheung and Ewald 2016), a known p120 and E-cadherin dependent process (Macpherson, Hooper et al. 2007, Kota, Terrell et al. 2019, Gritsenko, Atlasy et al. 2020). Remarkably, all of these dedicated metastatic processes are partly, if not wholly, dependent on the so-called “metastasis suppressor”, E-cadherin. Our data and conclusions by enlarge are in line with related evidence published recently by Ewald and colleagues for E-cadherin (Padmanaban et al., 2019).

## Materials and Methods

*Patient cohort and tissue samples*

A cohort of clinically characterized breast cancer patients with primary invasive ductal cancer diagnosed from 1991-2005 at the University Hospital Zurich was enrolled in the tissue microarray (TMA) study as described elsewhere (Theurillat, Ingold et al. 2007). Tumor grade was performed according to the modified Bloom and Richardson system (Bocker 2002, Tavassoeli 2003). Of this

cohort, invasive ductal carcinomas were studied. For clinicopathological parameters, see supplemental Table S1. Because 10% of the patients were followed-up >120 months, follow-up time was censored in all survival analyses presented in this article. The study was approved by the ethical committee of the Kanton of Zurich (reference number StV-12-2005).

*Immunohistochemistry on Patient Samples*

All antibodies were tested on a multi-tissue TMA for appropriate dilution and were used in a diagnostic protocol. Monoclonal antibodies to anti-p120 (BD Bioscience, clone 98/pp120, 1:200), and anti-E-cadherin (Cell Marque Lifescreen Ltd., Rocklin, CA, USA, clone EP700Y, 1:200), anti-Ki-67 (Dako, Glostrup, Denmark, clone MIB1, 1:20), anti-p63 (Thermo Scientific Lab Vision, Thermo Scientific, 4A4+Y4A3 (63P02), 1:200) were used. All immunohistochemical stains were performed on a Ventana Benchmark® platform (Ventana Medical Systems, Tucson, AZ, USA). The CC1 standard pretreatment with 60 min boiling in pH 8 Tris buffer (Ventana) was followed by incubation with primary mAb (dilution 1:200) for 60 min at room temperature (RT) and development with the Ultraview-HRP kit (Ventana/Roche), including incubation with respective secondary antibody for 30 min at RT. P120 antibody was diluted in Tris/BSA. For counterstains, hematoxylin was used. P120 immunoreactivity at the tumor cell membrane was semi-quantitatively evaluated applying a four-tiered system (score 0 negative, score 1-weak discontinuous expression, score 2-moderate continuous expression, and 3 score-strong continuous expression). Cytoplasmic p120 staining was scored as negative (score 0), weak (score 1), moderate (score 2) and strong (score 3). Scoring was done by three experienced pathologists (A. N., Z. V., V. T). Normal breast glands served as positive internal control and a standard for score 3. E-cadherin was evaluated at the tumor cell membrane as positive (strong expression) and negative (partial or complete loss of expression) cases (S. B.) Estrogen receptor status and HER2 FISH analysis were performed as described elsewhere (Theurillat, Ingold et al. 2007).

*Animals*

To generate mammary-specific p120 KO mice, p120f/f mice were backcrossed onto an FVB/NJ background and crossed with MMTV-cre#7 obtained from Dr. Muller on an FVB background (Andrechek, Hardy et al. 2000), (Andrechek, White et al. 2005, Perez-Moreno, Davis et al. 2006, Kurley, Bierie et al. 2012). p120 ablation in a mouse model of breast cancer was achieved by crossing the mammary-specific p120 KO mice with an FVB backcrossed version of MMTV-Polyoma Middle T (PyMT) model (Guy, Cardiff et al. 1992). All experiments involving animals were approved by the Vanderbilt University Institutional Animal Care and Use Committee.

*Immunohistochemistry/Immunofluorescence on mouse samples*

Fluorescent Immunostaining on tissue was performed as previously described (Perez-Moreno, Davis et al. 2006, Kurley, Bierie et al. 2012). Briefly, tissues were fixed in 10% formalin. Paraffin-embedded tissue sections were deparaffinized and rehydrated. Antigen retrieval was performed by boiling slides

in 10 mM Sodium Citrate pH 6.0 for 10 minutes. After blocking, slides were incubated in primary and secondary antibody overnight and for 2 hours, respectively. Primary antibodies against the following were utilized: p120 (F1αSH 0.8μg/mL), E-cadherin (0.5 μg/mL, BD Biosciences), β-catenin (1:800, Sigma-Aldrich), Keratin 8 (TROMA-I 1:1000 0.2μg/mL University of Iowa Hybridoma Core), F4/80 (1:200, AbDSerotec- requires trypsin antigen retrieval), SMA (0.2μg/mL Sigma-Aldrich), Meca32 (1:100, BD Biosciences). Secondary antibodies (1:500, Invitrogen) were conjugated to either Alexa dye 488, 594, or 647. Sections were mounted with Prolong Gold Antifade Mounting Medium (Invitrogen, Carlsbad, California, USA). Tissue processing, hematoxylin and eosin (H&E) staining, and immunohistochemsitry for CD31 (1:100, Dianova) and CD3 (1:600, Santa Cruz Biotechnology) was performed by the Vanderbilt Translational Pathology Shared Resource Core. TUNEL staining assays were performed as per the manufacturer's instructions with the following modification: antigen retrieval for 10 minutes in proteinase K (Millipore, Danvers, Massachusetts, USA). Staining was visualized using an Axioplan 2 microscope (Zeiss, Oberkochen, Germany). Images were collected with either an Olympus QColor 3TM digital camera or a Hamamatsu Orca ER fluorescent camera and processed using MetaMorph software.

*Cell Immunofluorescence*

Cells were plated on glass coverslips and fixed in 3% paraformaldehyde for 30 minutes. After PBS washes, cells were permeabilized in PBS with 0.2% TritonX-100 for 5 minutes. After more PBS washes, non-specific binding was blocked using PBS with 3% nonfat milk. Cells were incubated in primary antibody for 30 minutes, washed, and incubated in secondary antibody for 30 minutes. After 3 PBS washes, nuclei were stained using Hoechst dye. Coverslips were coated in ProLong gold (Invitrogen) and mounted on glass slides. Quantification of staining was assessed in n=6 mice per genotype, 1 section encompassing random pieces of tissue, six images per section. When possible, p120 negative regions for KO animals were determined using co-IF.

*Generation and Manipulation of PyMT-derived Cell Lines*

Tumor tissue was collected under sterile conditions, minced into 1mm size pieces, and incubated in digest media [DMEM:F12, 1% antibiotic/antimycotic, 100 units/mL hyaluronidase, 3 mg/mL collagenase A, gentamycin] for 3-4 hours with agitation at 37°C. Cells were pelleted at 1000 RPM and washed 5 times in PBS supplemented with 5% adult bovine serum. Fibroblasts were removed by resuspending the pellet in low serum media and plating the material on a sterile petri dish. After 1 hour in the incubator, cells not attached to the dish were spun down and resuspended in full growth media [DMEM:F-12, 5% adult bovine serum, insulin, progesterone, 17-b-estradiol, EGF, 1% antibiotic/antimycotic, gentamicin]. Cells were plated onto collagen-coated plates and allowed to adhere for 48 hours before media changing. Cell lines were established by passaging cells at least 15 times prior to experimental use after which point they were grown in DMEM supplemented with 10% FBS. To generate matched cell lines with and without p120, cell lines were transduced with

lentiviral constructs expressing non-targeting shRNA (control) or Cre-recombinase (p120 KO) and then cells were selected for by puromycin treatment.

*Wound Healing Assays*

PyMT-derived cells were plated to confluence and scratched with a P200 tip to generate the wound. Cells were rinsed with PBS, covered in growth media, and imaged at six regions per scratch every 6 hours. Images were acquired using an Axiovert 200M microscope (Zeiss) and processed using MetaMorph software.

*Transwell Invasion Assays*

Matrigel-coated transwells were equilibrated by the manufacturer's instructions. Cells were then plated in serum-free media in the top well and promoted to invade toward 10% media in the bottom chamber. After 24-48 hours, transwells were fixed and stained using a Diff-Quik staining kit (Allegiance). Ten random fields of view per transwell were analyzed. For macrophage invasion assays, intraperitoneal injections with 2 mL thioglycolate were performed using a 27G needle. After 4 days, the abdominal cavity was filled with PBS, and peritoneal macrophages were isolated. Macrophages were pelleted and resuspended in serum- free media and immediately used for invasion assays as described above. To generate the stimulus for macrophage invasion, PyMT-derived cells were grown in 3D matrigel cultures for at least seven days. Serum-free media was added to the cultures, collected after 24 hours, and used for invasion induction of macrophages.

*Western Blot Analysis*

Protein was isolated as previously described (Mariner et al., 2004). Briefly, cells were washed with PBS, lysed in RIPA buffer [50 mM Tris (pH 7.4), 150 mM NaCl, 1%Nonidet P-40, 0.5% Deoxycholic Acid, 0.1% sodium dodecyl sulfate] containing inhibitors [1mM phenylmethylsulfonyl fluoride, 5 µg/mL leupeptin, 2 µg/mL aprotinin, 1mM sodium orthovanadate, 1mM EDTA, 50mM NaF, 40mM B-glycerophasphate] and spun at 14,000g at 4°C for 5 minutes. Cleared total protein was quantified using a bicinchoninic acid assay (Pierce, Rockford, Illinois, USA). 20 µg of protein per sample were boiled in 2X Laemmli sample buffer and separated by SDS-polyacrylamide gel electrophoresis. Proteins were transferred to nitrocellulose (PerkinElmer, Waltham, Massachusetts, USA). Non-specific binding was blocked by incubating membranes in 3% nonfat milk in Tris-buffered saline and Odyssesy blocking buffer (LI-COR, Lincoln, Nebraska USA) prior to the addition of primary and secondary antibodies, respectively. Anti-p120/pp120 (0.1µg/mL, BD Biosciences), anti-E-cadherin (0.1µg/mL, BD Biosciences), anti-tubulin/DM1α (1:1000, Sigma-Aldrich), anti-N-cadherin (0.8µg/mL 13A9, Millipore), and anti-P-cadherin (1:250, BD Biosciences) antibodies were used. The Odyssey system was used for the detection of secondary goat anti-mouse IgG IRDye 800CW antibodies (1:10,000 LI-COR).

*Orthotopic Transplant*

$1X10^6$ cells were suspended in 50 µL of 1:1 type I collagen (1.19 mg/mL final concentration) to neutralization solution [100mM Hepes in 2X PBS pH 7.3]. Plugs were allowed to solidify for 1 hour in the incubator and then covered in growth media. The following day plugs were transplanted into the cleared fat mammary fat pads of 3 week-old female mice. Tumor growth was assessed by caliper and tumors and lungs were collected 5 weeks after transplant.

*Tail Vein Injections and Lung Whole Mount*

PyMT-derived cells were trypsinized, pelleted, and washed 3 times in PBS. After passage through a 70µM strainer, $1x10^6$ cells per 100 µL were injected into the tail vein of mice. After four weeks, mice were sacrificed, and lungs were collected. Lungs were analyzed by whole mount and tumor burden analysis. Tumor burden was quantified as a percent of metastases area to total lung area at three depths per lung. For lung whole mount, lungs were inflated with formalin and fixed overnight. Lungs were then dehydrated in progressive increasing amounts of ethanol and cleared overnight in Histoclear. Rehydration the next day was followed by staining in Mayer's hematoxylin. After destain steps in 1% HCl solution and water, lungs were dehydrated and cleared once again. Analysis of lung metastases was performed using a dissecting scope and an Olympus QColor 3TM digital camera.

*Whole Tumor*

Tumors were collected, minced, and incubated in digest media [RPMI with 1 mg/mL collagenase I, 1 mg/mL dispase II] for 2 hours at 37°C. Tumor material was then pressed through a 70 µM cell strainer in 10 mL cold PBS and repeated for a total of 50 mL PBS. Tumor cells were then treated with 10 µL of 5MU/mL DNAseI for 5 minutes at room temperature. Cells were pelleted at 300g to remove DNAse treatment. Red blood cells were removed from tumor preparations using lysis buffer. Cells were washed with PBS, strained, and then counted in the presence of trypan blue. Each sample of 5x10^6 cells per 100 µL flow buffer [PBS, 0.5% BSA, 2mM EDTA] was treated with Fc block and then incubated in antibodies conjugated to compatible fluorophore combinations for 30 minutes on ice. All antibodies were purchased through eBioscience. After 2 washes with flow buffer, cells were analyzed by flow cytometry by the Vanderbilt Flow Cytometry Shared Resource Core.

*Anchorage Independent and 3D Matrigel Growth*

For anchorage-independent growth assays, six well-dishes were coated with a layer of 0.7% low gelling temperature agarose. 5x10^3 PyMT-derived cells suspended in 0.35% agarose were plated per well and covered in 2 mL growth media. After 3.5 weeks of growth, colonies were imaged using an inverted microscope. For 3D growth assays, 35 mm tissue culture dishes were coated with 500 µL of Matrigel. 7x10^5 PyMT-derived cells were plated in growth media supplemented with 2% Matrigel.

*qRT-PCR on Macrophages*

Total RNA was extracted from sorted CD45+CD11b+F4/80+ cells from tumors of d54 PyMT control and p120 KO mice (n=3 per genotype) using QIAshredder columns and RNeasy mini kit (Qiagen). cDNA was synthesized using Invitrogen Superscript Firststrand synthesis system for RT-PCR (Invitrogen). Primers specific for iNOS, TNFα, IL-12, IL-6, IL-1b, VEGF, MMP2, MMP9, MMP13, CXCL1, and IL-10 were used and the relative gene expression was determined using ABI PRISM 7900HT Sequence Detection System (PE Applied Biosystems). The comparative threshold cycle method was used to calculate gene expression normalized to β actin.

*Circulating Tumor Cell Assays*

Fifty-four days after initial palpation mice were euthanized (n=4 per genotype) and whole blood was collected in a heparinized needle. Each well of a 6-well dish was coated in 1:1 mix of Matrigel and DMEM supplemented with 10% FBS. After Matrigel solidification, 500 µL of whole blood was plated per 6-well dish and covered in 2 mL media. After 48 hours, cultures were washed with PBS. Red blood cells were removed with lysis buffer [155 mM NH4Cl, 12mM NaHCO3, 0.1 mM EDTA] and then washed away with PBS. Colonies were then allowed to grow for 7-10 days with media changes every 3-4 days. Colonies were counted in 5 random 2.5x fields and 10 random 10x fields. For qRT-PCR experiments, RNA was isolated from whole blood and RT-PCR assays conducted were performed as previously described (Connelly et al., 2011).

*Statistical Analysis*

Statistical analyses for non-clinical data were performed using GraphPad Prism (GraphPad La Jolla, California, USA) as described in figure legends. For assays with or without normal distribution, two-tailed Student's t-tests or Mann-Whitney tests were performed, respectively. For clinical samples, associations of staining intensity with clinicopathological parameters were done by descriptive statistics (cross tables, two-tailed Fisher's exact test, and two-tailed $\chi^2$ test for trends (linear-by-linear). For correlation significance between immunohistochemical and fluorescence in-situ based markers, Kendall's tau b for non-parametric correlations was used. P-values<0.05 were considered significant. Correlations of p120 expression with overall survival were calculated

**Acknowledgments**

We are grateful to members of the Reynolds laboratory, Dr. Carlos L. Arteaga and laboratory, Dr. David Vaught, and Dr. Andrew Smith for helpful discussions of this work. We would like to acknowledge Martina Storz, Susanne Dettwiler, and Jasmin Roth for their excellent technical assistance. Some of the text and figures in this paper formed part of Sarah Jean Kurley's PhD thesis in the Department of Cancer Biology at Vanderbilt University in 2012.

**Competing Interests:** The authors have no competing interest to declare.

**Funding:** Technical support was provided by the following Vanderbilt University Core Resources: VUMC Cell Imaging Shared Resource (CA68485, DK20593, DK58404, HD15052, DK59637 and EY08126); Translational Pathology Shared Resource; and VMC Flow Cytometry Shared Resource (P30 CA68485, DK058404). This work was supported by NIH R01 CA111947 and NIH R01 CA55724 to A.B.R., NIH 2PO1CA099031-06A1 to W.J.M., and Predoctoral Trainee Award BC083306 to S.J.K. Funding was also received through the Vanderbilt Cancer Center Support Grant [NIH P30 CA068485] and a Pilot Grant to A.B.R. through the Vanderbilt Breast SPORE [NIH P50 CA98131].

**References:**


**Andrechek, E. R., W. R. Hardy, P. M. Siegel, M. A. Rudnicki, R. D. Cardiff and W. J. Muller** (2000). "Amplification of the neu/erbB-2 oncogene in a mouse model of mammary tumorigenesis." Proc Natl Acad Sci U S A **97**(7): 3444-3449.

**Andrechek, E. R., D. White and W. J. Muller** (2005). "Targeted disruption of ErbB2/Neu in the mammary epithelium results in impaired ductal outgrowth." Oncogene **24**(5): 932-937.

**Berx, G., A. M. Cleton-Jansen, F. Nollet, W. J. de Leeuw, M. van de Vijver, C. Cornelisse and F. van Roy** (1995). "E-cadherin is a tumour/invasion suppressor gene mutated in human lobular breast cancers." EMBO J **14**(24): 6107-6115.

**Bocker, W**. (2002). "[WHO classification of breast tumors and tumors of the female genital organs: pathology and genetics]." Verh Dtsch Ges Pathol 86: 116-119.

**Brabletz, T.** (2012). "EMT and MET in metastasis: where are the cancer stem cells?" Cancer Cell **22**(6): 699-701.

**Chetty, R. and S. Serra** (2008). "Nuclear E-cadherin immunoexpression: from biology to potential applications in diagnostic pathology." Adv Anat Pathol **15**(4): 234-240.

**Cheung, K. J. and A. J. Ewald (2016). "A collective route to metastasis: Seeding by tumor cell clusters."** Science **352**(6282): 167-169.

**Davis, M. A. and A. B. Reynolds** (2006). "Blocked acinar development, E-cadherin reduction, and intraepithelial neoplasia upon ablation of p120-catenin in the mouse salivary gland." Dev Cell **10**(1): 21-31.

**DeNardo, D. G. and L. M. Coussens** (2007). "Inflammation and breast cancer. Balancing immune response: crosstalk between adaptive and innate immune cells during breast cancer progression." Breast Cancer Res **9**(4): 212.

**Derksen, P. W., T. M. Braumuller, E. van der Burg, M. Hornsveld, E. Mesman, J. Wesseling, P. Krimpenfort and J. Jonkers** (2011). "Mammary-specific inactivation of E-cadherin and p53 impairs functional gland development and leads to pleomorphic invasive lobular carcinoma in mice." Dis Model Mech **4**(3): 347-358.

**Dillon, D. A., T. D'Aquila, A. B. Reynolds, E. R. Fearon and D. L. Rimm** (1998). "The expression of p120ctn protein in breast cancer is independent of alpha- and beta-catenin and E-cadherin." Am J Pathol **152**(1): 75-82.

**El Sharouni, M. A., E. L. Postma and P. J. van Diest** (2017). "Correlation between E-cadherin and p120 expression in invasive ductal breast cancer with a lobular component and MRI findings." Virchows Arch **471**(6): 707-712.

**Fan, X., S. Jin, Y. Li, P. A. Khadaroo, Y. Dai, L. He, D. Zhou and H. Lin** (2019). "Genetic And Epigenetic Regulation Of E-Cadherin Signaling In Human Hepatocellular Carcinoma." Cancer Manag Res **11**: 8947-8963.

**Gritsenko, P. G., N. Atlasy, C. E. J. Dieteren, A. C. Navis, J. H. Venhuizen, C. Veelken, D. Schubert, A. Acker-Palmer, B. A. Westerman, T. Wurdinger, W. Leenders, P. Wesseling, H. G. Stunnenberg and P. Friedl** (2020). "p120-catenin-dependent collective brain infiltration by glioma cell networks." Nat Cell Biol **22**(1): 97-107.

**Gunasinghe, N. P., A. Wells, E. W. Thompson and H. J. Hugo** (2012). "Mesenchymal-epithelial transition (MET) as a mechanism for metastatic colonisation in breast cancer." Cancer Metastasis Rev **31**(3-4): 469-478.

**Guy, C. T., R. D. Cardiff and W. J. Muller** (1992). "Induction of mammary tumors by expression of polyomavirus middle T oncogene: a transgenic mouse model for metastatic disease." Mol Cell Biol **12**(3): 954-961.

**Hendley, A. M., Y. J. Wang, K. Polireddy, J. Alsina, I. Ahmed, K. J. Lafaro, H. Zhang, N. Roy, S. G. Savidge, Y. Cao, M. Hebrok, A. Maitra, A. B. Reynolds, M. Goggins, M. Younes, C. A.**

**Iacobuzio-Donahue, S. D. Leach and J. M. Bailey** (2016). "p120 Catenin Suppresses Basal Epithelial Cell Extrusion in Invasive Pancreatic Neoplasia." Cancer Res **76**(11): 3351-3363.

**Hernandez-Martinez, R., N. Ramkumar and K. V. Anderson** (2019). "p120-catenin regulates WNT signaling and EMT in the mouse embryo." Proc Natl Acad Sci U S A **116**(34): 16872-16881.

**Hu, G.** (2012). "p120-Catenin: a novel regulator of innate immunity and inflammation." Crit Rev Immunol **32**(2): 127-138.

**Huang, B., M. K. Jolly, M. Lu, I. Tsarfaty, E. Ben-Jacob and J. N. Onuchic** (2015). "Modeling the Transitions between Collective and Solitary Migration Phenotypes in Cancer Metastasis." Sci Rep **5**: 17379.

**Jeanes, A., C. J. Gottardi and A. S. Yap** (2008). "Cadherins and cancer: how does cadherin dysfunction promote tumor progression?" Oncogene **27**(55): 6920-6929.

**Jones, J., H. Wang, B. Karanam, S. Theodore, W. Dean-Colomb, D. R. Welch, W. Grizzle and C. Yates** (2014). "Nuclear localization of Kaiso promotes the poorly differentiated phenotype and EMT in infiltrating ductal carcinomas." Clin Exp Metastasis **31**(5): 497-510.

**Kang, Y. and K. Pantel** (2013). "Tumor cell dissemination: emerging biological insights from animal models and cancer patients." Cancer Cell **23**(5): 573-581.

**Kim, S. A., C. Y. Tai, L. P. Mok, E. A. Mosser and E. M. Schuman** (2011). "Calcium-dependent dynamics of cadherin interactions at cell-cell junctions." Proc Natl Acad Sci U S A **108**(24): 9857-9862.

**Kota, P., E. M. Terrell, D. A. Ritt, C. Insinna, C. J. Westlake and D. K. Morrison** (2019). "M-Ras/Shoc2 signaling modulates E-cadherin turnover and cell-cell adhesion during collective cell migration." Proc Natl Acad Sci U S A **116**(9): 3536-3545.

**Kurley, S. J., B. Bierie, R. H. Carnahan, N. A. Lobdell, M. A. Davis, I. Hofmann, H. L. Moses, W. J. Muller and A. B. R**eynolds (2012). "p120-catenin is essential for terminal end bud function and mammary morphogenesis." Development **139**(10): 1754-1764.

**Lin, E. Y., J. G. Jones, P. Li, L. Zhu, K. D. Whitney, W. J. Muller and J. W. Pollard** (2003). "Progression to malignancy in the polyoma middle T oncoprotein mouse breast cancer model provides a reliable model for human diseases." Am J Pathol **163**(5): 2113-2126.

**Macpherson, I. R., S. Hooper, A. Serrels, L. McGarry, B. W. Ozanne, K. Harrington, M. C. Frame, E. Sahai and V. G. Brunton** (2007). "p120-catenin is required for the collective invasion of squamous cell carcinoma cells via a phosphorylation-independent mechanism." Oncogene **26**(36): 5214-5228.

**Mastracci, T. L., S. Tjan, A. L. Bane, F. P. O'Malley and I. L. Andrulis** (2005). "E-cadherin alterations in atypical lobular hyperplasia and lobular carcinoma in situ of the breast." Mod Pathol **18**(6): 741-751.

**Muraoka, R. S., A. E. Lenferink, B. Law, E. Hamilton, D. M. Brantley, L. R. Roebuck and C. L. Arteaga** (2002). "ErbB2/Neu-induced, cyclin D1-dependent transformation is accelerated in p27-haploinsufficient mammary epithelial cells but impaired in p27-null cells." Mol Cell Biol **22**(7): 2204-2219.

**Nakopoulou, L., H. Gakiopoulou-Givalou, A. J. Karayiannakis, I. Giannopoulou, A. Keramopoulos, P. Davaris and M. Pignatelli** (2002). "Abnormal alpha-catenin expression in invasive breast cancer correlates with poor patient survival." Histopathology **40**(6): 536-546.

**Oas, R. G., K. Xiao, S. Summers, K. B. Wittich, C. M. Chiasson, W. D. Martin, H. E. Grossniklaus, P. A. Vincent, A. B. Reynolds and A. P. Kowalczyk** (2010). "p120-Catenin is required for mouse vascular development." Circ Res **106**(5): 941-951.

**Ozawa, M**. (2003). "p120-independent modulation of E-cadherin adhesion activity by the membrane-proximal region of the cytoplasmic domain." J Biol Chem **278**(46): 46014-46020.

**Peglion, F., F. Llense and S. Etienne-Manneville** (2014). "Adherens junction treadmilling during collective migration." Nat Cell Biol **16**(7): 639-651.

**Perez-Moreno, M., M. A. Davis, E. Wong, H. A. Pasolli, A. B. Reynolds and E. Fuchs** (2006). "p120-catenin mediates inflammatory responses in the skin." Cell **124**(3): 631-644.

**Perez-Moreno, M., W. Song, H. A. Pasolli, S. E. Williams and E. Fuchs** (2008). "Loss of p120 catenin and links to mitotic alterations, inflammation, and skin cancer." Proc Natl Acad Sci U S A **105**(40): 15399-15404.

**Reichert, M., B. Bakir, L. Moreira, J. R. Pitarresi, K. Feldmann, L. Simon, K. Suzuki, R. Maddipati, A. D. Rhim, A. M. Schlitter, M. Kriegsmann, W. Weichert, M. Wirth, K. Schuck, G. Schneider, D. Saur, A. B. Reynolds, A. J. Klein-Szanto, B. Pehlivanoglu, B. Memis, N. V. Adsay and A. K. Rustg**i (2018). "Regulation of Epithelial Plasticity Determines Metastatic Organotropism in Pancreatic Cancer." Dev Cell **45**(6): 696-711 e698.

**Richert, M. M., P. A. Phadke, G. Matters, D. J. DiGirolamo, S. Washington, L. M. Demers, J. S. Bond, A. Manni and D. R. Welch** (2005). "Metastasis of hormone-independent breast cancer to lung and bone is decreased by alpha-difluoromethylornithine treatment." Breast Cancer Res **7**(5): R819-827.

**Saijo, Y., G. Sato, K. Usui, M. Sato, M. Sagawa, T. Kondo, Y. Minami and T. Nukiwa (2001). "Expression** of nucleolar protein p120 predicts poor prognosis in patients with stage I lung adenocarcinoma." Ann Oncol **12**(8): 1121-1125.

**Sarrio, D., B. Perez-Mies, D. Hardisson, G. Moreno-Bueno, A. Suarez, A. Cano, J. Martin-Perez, C. Gamallo and J. Palacio**s (2004). "Cytoplasmic localization of p120ctn and E-cadherin loss characterize lobular breast carcinoma from preinvasive to metastatic lesions." Oncogene **23**(19): 3272-3283.

**Schackmann, R. C., S. Klarenbeek, E. J. Vlug, S. Stelloo, M. van Amersfoort, M. Tenhagen, T. M. Braumuller, J. F. Vermeulen, P. van der Groep, T. Peeters, E. van der Wall, P. J. van Diest, J. Jonkers and P. W. Derksen** (2013). "Loss of p120-catenin induces metastatic progression of breast cancer by inducing anoikis resistance and augmenting growth factor receptor signaling." Cancer Res **73**(15): 4937-4949.

**Schackmann, R. C., M. Tenhagen, R. A. van de Ven and P. W. Derksen** (2013). "p120-catenin in cancer - mechanisms, models and opportunities for intervention." J Cell Sci **126**(Pt 16): 3515-3525.

**Schackmann, R. C., M. van Amersfoort, J. H. Haarhuis, E. J. Vlug, V. A. Halim, J. M. Roodhart, J. S. Vermaat, E. E. Voest, P. van der Groep, P. J. van Diest, J. Jonkers and P. W. Derksen** (2011). "Cytosolic p120-catenin regulates growth of metastatic lobular carcinoma through Rock1-mediated anoikis resistance." J Clin Invest **121**(8): 3176-3188.

**Short, S. P., C. W. Barrett, K. R. Stengel, F. L. Revetta, Y. A. Choksi, L. A. Coburn, M. K. Lintel, E. M. McDonough, M. K. Washington, K. T. Wilson, E. Prokhortchouk, X. Chen, S. W. Hiebert, A. B. Reynolds and C. S. Williams** (2019). "Kaiso is required for MTG16-dependent effects on colitis-associated carcinoma." Oncogene **38**(25): 5091-5106.

**Short, S. P., J. Kondo, W. G. Smalley-Freed, H. Takeda, M. R. Dohn, A. E. Powell, R. H. Carnahan, M. K. Washington, M. Tripathi, D. M. Payne, N. A. Jenkins, N. G. Copeland, R. J. Coffey and A. B. Reynolds** (2017). "p120-Catenin is an obligate haploinsufficient tumor suppressor in intestinal neoplasia." J Clin Invest **127**(12): 4462-4476.

**Silvera, D., R. Arju, F. Darvishian, P. H. Levine, L. Zolfaghari, J. Goldberg, T. Hochman, S. C. Formenti and R. J. Schneider** (2009). "Essential role for eIF4GI overexpression in the pathogenesis of inflammatory breast cancer." Nat Cell Biol **11**(7): 903-908.

**Silvera, D. and R. J. Schneider** (2009). "Inflammatory breast cancer cells are constitutively adapted to hypoxia." Cell Cycle **8**(19): 3091-3096.

**Singhai, R., V. W. Patil, S. R. Jaiswal, S. D. Patil, M. B. Tayade and A. V. Patil** (2011). "E-Cadherin as a diagnostic biomarker in breast cancer." N Am J Med Sci **3**(5): 227-233.

**Smalley-Freed, W. G., A. Efimov, P. E. Burnett, S. P. Short, M. A. Davis, D. L. Gumucio, M. K. Washington, R. J. Coffey and A. B. Reynolds** (2010). "p120-catenin is essential for maintenance of barrier function and intestinal homeostasis in mice." J Clin Invest **120**(6): 1824-1835.

**Smalley-Freed, W. G., A. Efimov, S. P. Short, P. Jia, Z. Zhao, M. K. Washington, S. Robine, R. J. Coffey and A. B. Reynolds** (2011). "Adenoma formation following limited ablation of p120-catenin in the mouse intestine." PLoS One **6**(5): e19880.

**Stairs, D. B., L. J. Bayne, B. Rhoades, M. E. Vega, T. J. Waldron, J. Kalabis, A. Klein-Szanto, J. S. Lee, J. P. Katz, J. A. Diehl, A. B. Reynolds, R. H. Vonderheide and A. K. Rustgi** (2011). "Deletion of p120-catenin results in a tumor microenvironment with inflammation and cancer that establishes it as a tumor suppressor gene." Cancer Cell **19**(4): 470-483.

**Sun, Y., J. Zhang and L. Ma** (2014). "alpha-catenin. A tumor suppressor beyond adherens junctions." Cell Cycle **13**(15): 2334-2339.

**Talvinen, K., J. Tuikkala, M. Nykanen, A. Nieminen, J. Anttinen, O. S. Nevalainen, S. Hurme, T. Kuopio and P. Kronqvist** (2010). "Altered expression of p120catenin predicts poor outcome in invasive breast cancer." J Cancer Res Clin Oncol **136**(9): 1377-1387.

**Tavassoeli, F. a. D. P. (2003). "Tumors of the Breast and Female Genital Organs (IARC WHO** Classification of Tumours)."

**Theurillat, J. P., F. Ingold, C. Frei, A. Zippelius, Z. Varga, B. Seifert, Y. T. Chen, D. Jager, A. Knuth and H. Moch** (2007). "NY-ESO-1 protein expression in primary breast carcinoma and metastases: correlation with CD8+ T-cell and CD79a+ plasmacytic/B-cell infiltration." Int J Cancer **120**(11): 2411-2417.

**Theveneau, E. and R. Mayor** (2012). "Cadherins in collective cell migration of mesenchymal cells." Curr Opin Cell Biol **24**(5): 677-684.

**Thiery, J. P., B. Boyer, G. Tucker, J. Gavrilovic and A. M. Valles** (1988). "Adhesion mechanisms in embryogenesis and in cancer invasion and metastasis." Ciba Found Symp **141**: 48-74.

**Thoreson, M. A., P. Z. Anastasiadis, J. M. Daniel, R. C. Ireton, M. J. Wheelock, K. R. Johnson, D. K. Hummingbird and A. B. Reynolds** (2000). "Selective uncoupling of p120(ctn) from E-cadherin disrupts strong adhesion." J Cell Biol **148**(1): 189-202.

**Valastyan, S. and R. A. Weinberg** (2011). "Tumor metastasis: molecular insights and evolving paradigms." Cell **147**(2): 275-292.

**VanderVorst, K., C. A. Dreyer, S. E. Konopelski, H. Lee, H. H. Ho and K. L. Carraway, 3rd** (2019). "Wnt/PCP Signaling Contribution to Carcinoma Collective Cell Migration and Metastasis." Cancer Res **79**(8): 1719-1729.

**Vos, C. B., A. M. Cleton-Jansen, G. Berx, W. J. de Leeuw, N. T. ter Haar, F. van Roy, C. J. Cornelisse, J. L. Peterse and M. J. van de Vijver** (1997). "E-cadherin inactivation in lobular carcinoma in situ of the breast: an early event in tumorigenesis." Br J Cancer **76**(9): 1131-1133.

**Wagner, W., C. Roderburg, F. Wein, A. Diehlmann, M. Frankhauser, R. Schubert, V. Eckstein and A. D. Ho** (2007). "Molecular and secretory profiles of human mesenchymal stromal cells and their abilities to maintain primitive hematopoietic progenitors." Stem Cells **25**(10): 2638-2647.

**Wehrendt, D. P., F. Carmona, A. E. Gonzalez Wusener, A. Gonzalez, J. M. Martinez and C. O. Arregui** (2016). "P120-Catenin Regulates Early Trafficking Stages of the N-Cadherin Precursor Complex." PLoS One **11**(6): e0156758.

**Wells, A., C. Yates and C. R. Shepard** (2008). "E-cadherin as an indicator of mesenchymal to epithelial reverting transitions during the metastatic seeding of disseminated carcinomas." Clin Exp Metastasis **25**(6): 621-628.

**Wijnhoven, B. P., M. Pignatelli, W. N. Dinjens and H. W. Tilanus** (2005). "Reduced p120ctn expression correlates with poor survival in patients with adenocarcinoma of the gastroesophageal junction." J Surg Oncol **92**(2): 116-123.

**Figures**

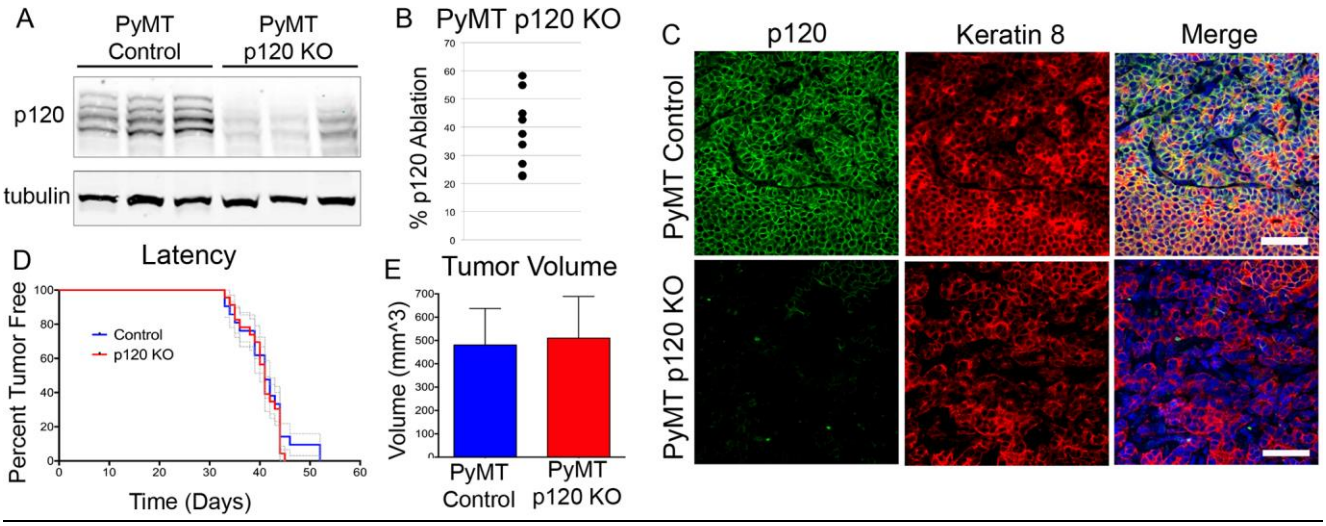


Figure 1: Latency and tumor volume are not altered by mosaic ablation of p120 in PyMT-induced mammary tumors

(A-C) Characterization of p120 status in tumors from control (MMTV-PyMT; MMTV-Cre) and p120 KO (MMTV-PyMT; MMTV-Cre; $p120^{fl/fl}$) mice. The p120 KO MMTV-PyMT p120 status in knockout and control mice was assessed by Western blotting and immunofluorescence. The proportion p120 KO cells in primary mammary tumors was estimated by p120 immunofluorescence staining of tumors from eight MMTV-Cre; p120fl/fl; MMTV-PyMT mice euthanized 54 days post palpation. Each point represents the percentage of carcinoma cells exhibiting p120 ablation averaged across three sections of random tumor sample per mouse. (D) Control and p120 ablated mice were monitored for tumors by palpation (n=21 WT blue, n=23 p120KO red). This n of >20 gives sufficient power (~90%) to detect significant differences. No difference in latency was observed using a log-rank test. (E) The volumes of all ten mammary tumors per mouse were approximated by calipering (h*l*w = approx. volume) at 54 days post palpation. Average volumes per mouse are shown. Error bars = standard deviation (n=6 WT blue, n=5 p120KO red). No significant difference was observed using a Mann-Whitney test.

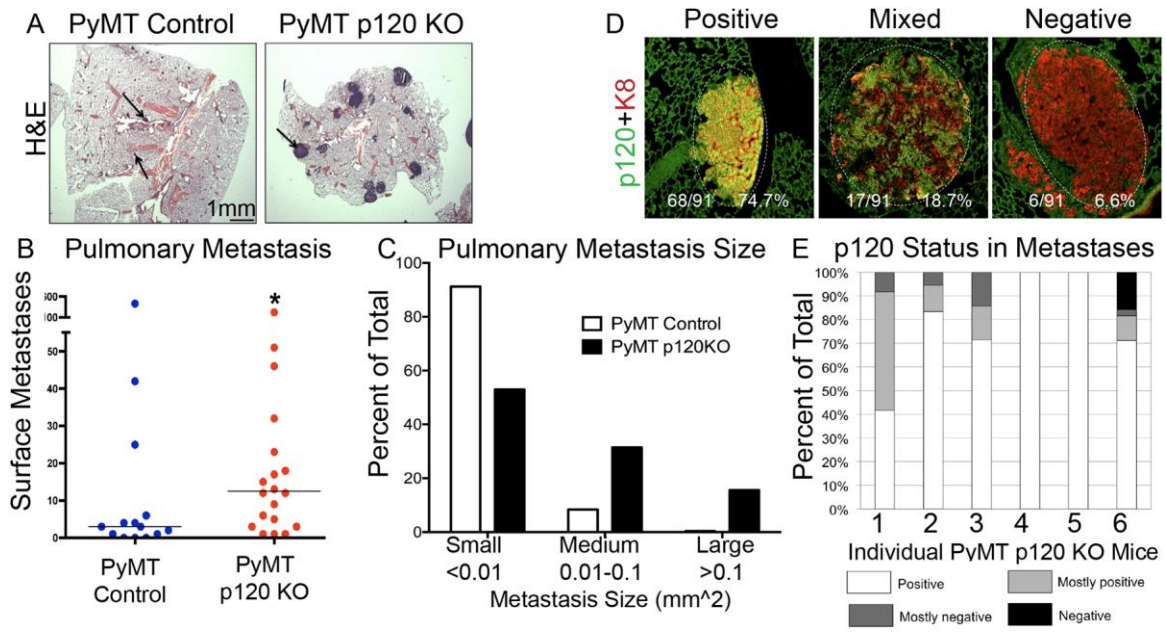


Figure 2. Primary tumor p120 ablation increases quantity and size of pulmonary metastases while selecting against p120 null cells

(A) Representative metastasis size is shown in lung sections stained with H&E. (B) Visible (surface) lung metastases were quantified by Hematoxylin staining performed on cleared lung whole mounts removed 54 days post tumor palpation. Mann-Whitney test *p<0.05 (C) Metastasis size was measured on lung sections stained with H&E. and binned into the described sizes. n=8 PyMT Control and n=12 PyMT p120KO mouse lungs were analyzed (D, E) Lungs from PyMT p120 knock out mice were stained for p120 and keratin 8 by immunofluorescence. After identification of PyMT cells by keratin 8 positivity, lung metastases were analyzed for p120 status. (D) Representative examples of pulmonary metastases stained for p120 and keratin 8. Collective binning data from 91 metastases from 6 PyMT p120KO mice are show (E) All visible metastases from n=6 PyMT p120 KO mice were assessed and binned into positive (white), mostly positive (light grey), mostly negative (dark grey), and negative (black). Data shown by each individual mouse.

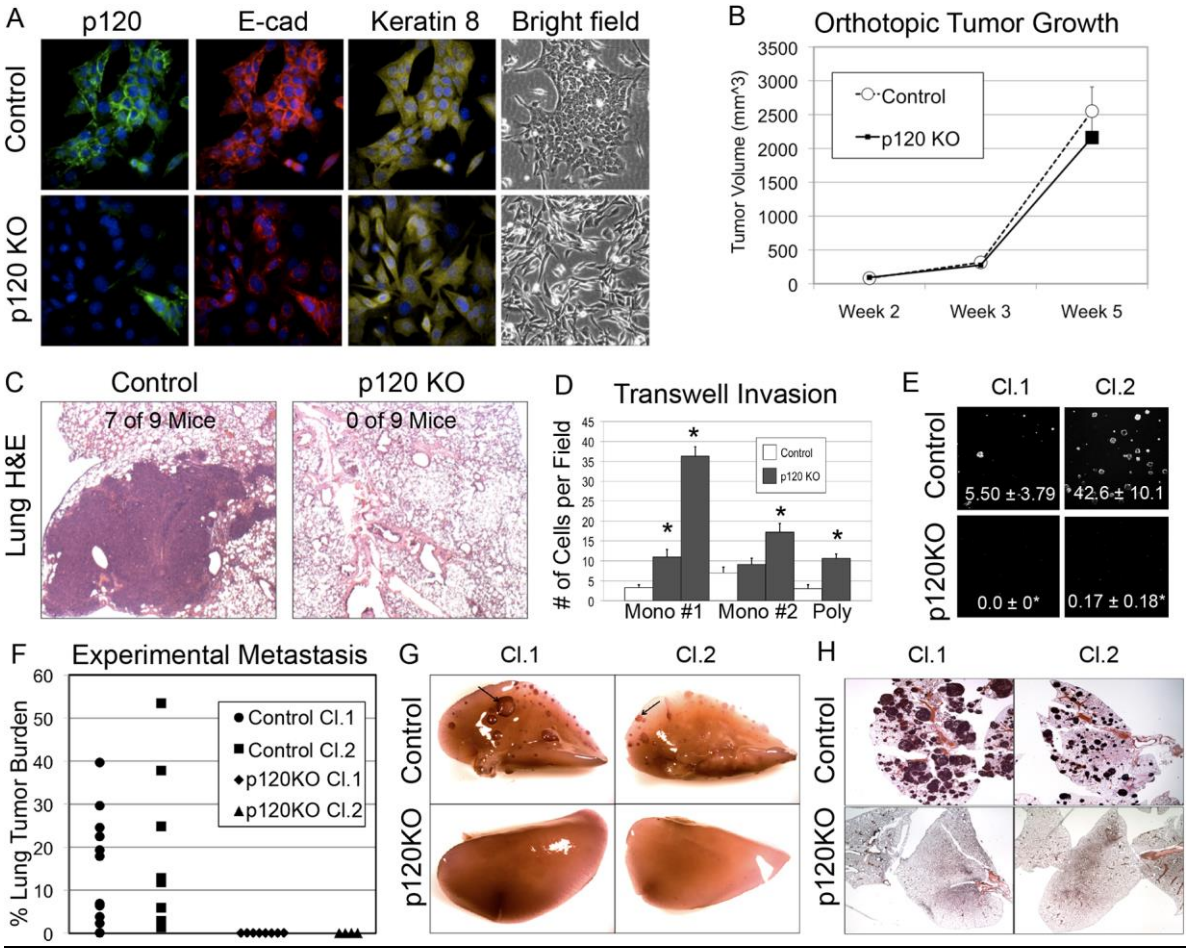


Figure 3. p120 ablation induces invasion but blocks pulmonary colonization

Cell lines were generated from MMTV-PyMT; p120f/f mice and were infected with empty or Cre expressing retrovirus to generate control or KO cells. (A) Co-immunofluorescence for p120, E-cadherin, and Keratin 8 confirms a predominantly p120 negative, keratin positive polyclonal population. KO cells are fibroblastic on plastic compared to cobblestone, epithelial control cells as evidenced by bright field imaging. (B) $1x10^6$ polyclonal cells expressing empty or Cre-recombinase vector were injected into the orthotopic site. Tumor growth of control and p120 KO cells transplanted into the orthotopic site of nude mice was monitored by calipers. (C) After 5 weeks, pulmonary metastases were assessed by H&E staining of lung sections. Control cells, but not KO cells metastasize to the lungs when transplanted into mammary glands of nude mice. Representative H&E stained sections of pulmonary tissue are shown above. The arrow denotes a metastasis. (D) In vitro invasion assays were performed using three independently derived PyMT cell lines (2 monoclonal and 1 polyclonal) infected with control or Cre lentivirus. Ten random fields of view per transwell were assessed after 36 hours. Student's t-test *$p<0.001$. Assays were performed two independent times and a representative graph is shown. (E) PyMT-derived cell lines were grown in agar for 3.5 weeks. Representative images at 2.5x magnification are shown. Quantification of growth in soft agar from two independent experiments is represented as average number of colonies per full field +/- standard deviation. *$p<0.01$ Student's t-test KO compared to either control. (F-H) PyMT-derived cells were

injected into the tail veins of female mice and assayed for lung tumor burden after 4 weeks. (F) Quantification of tumor burden in H&E stained sections. Mann-Whitney *p<0.01. Representative lung whole mount images (G) and H&E stained lung sections (H) are shown. Arrows denote metastases.

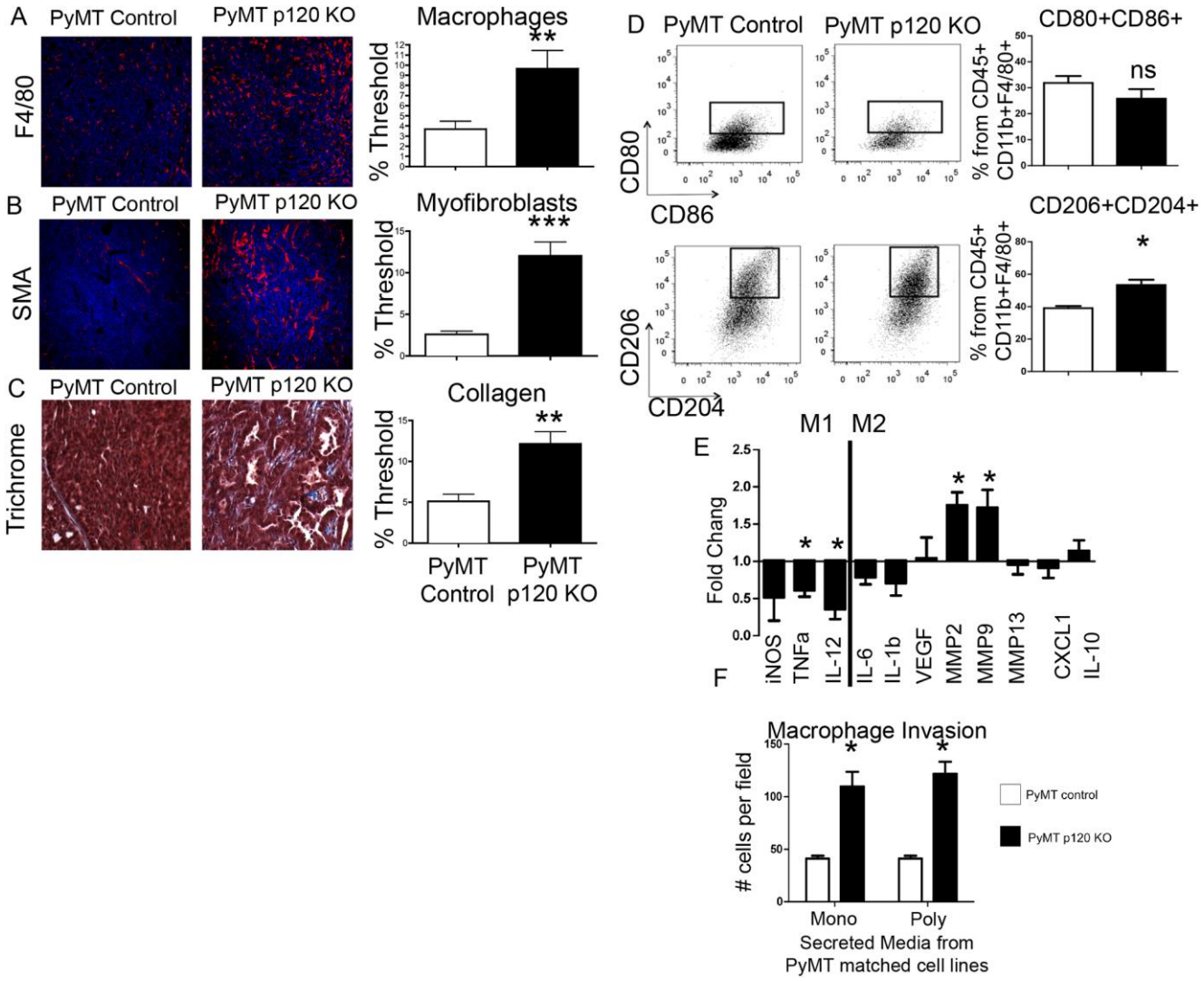


Figure 4. p120 ablation induces infiltration of M2 macrophages

(A-C) PyMT tumor sections were immuno-stained for F4/80 (A) or SMA (B) to detect macrophages and myofibroblasts, respectively. Nuclei are stained with Hoechst dye. To detect collagen, sections were stained with trichrome blue (C). n=6 mice per genotype with 6 random 20x images per single section were assessed. Mann-Whitney test: ***$p<0.0001$, **$p<0.01$. White bars are PyMT Control and black bars are PyMT p120 KO. Three regions of random tumor sample per mouse were assayed (n=5 per genotype) (D) Flow cytometry analysis of CD45+CD11b+F4/80+ cells in tumor tissue for cell surface markers of M1 (top, CD80+CD86+) and M2 (bottom, CD206+CD204+) phenotype. Representative FACS plots of macrophage numbers in tumor tissue. Plots are gated as CD45+DAPI-. Mann Whitney *$p>0.05$ .

(E) Quantitative RT-PCR on CD45+CD11b+F4/80+ cells from PyMT Control and PyMT p120 KO tumor tissues sorted by FACS Aria and converted to cDNA. Data are shown as fold over control.

(F) Macrophage invasion assay. Monoclonal or polyclonal-matched PyMT-derived cell lines were grown in 3D cultures. After establishment of colonies, serum free media was added and collected after 24 hours. Peritoneal macrophages were derived and plated onto Matrigel-coated transwells.

Macrophages were allowed to invade for 48 hours toward control or p120 KO cell secreted media. This graph is representative of two replicates. 10 fields per transwell were assessed for number of cells per field. *$p<0.05$ Student's t-test.

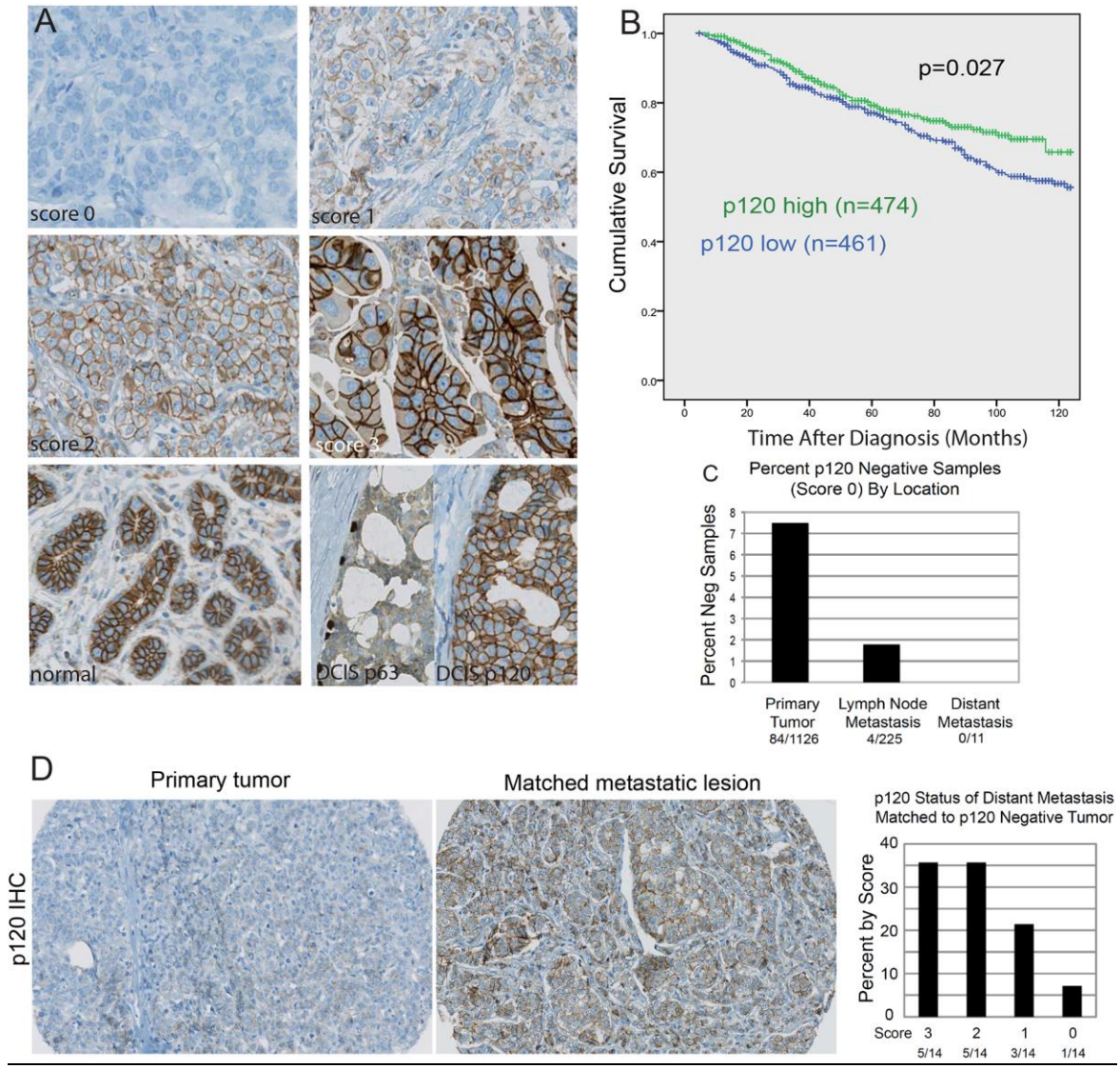


Figure 5. p120 expression in invasive breast cancer metastasis

(A) Representative examples of p120 expression in invasive ductal breast cancer (scores 0-3), normal breast glands and DCIS (p63 staining for myoepithelial cells) using IHC. (B) Kaplan-Meier curve illustrates a significantly shorted overall survival (censored at 120 months) for the patient group with altered p120 expression ("p120 low" scores 0-2) compared to "p120 high" expression (score 3), p=0.027. (C) Distribution of p120 negative samples by location of source tissue. (D) Representative IHC images of p120 negative samples (n=14) and matched metastatic disease. Graph denotes distribution of p120 status in matched metastases of p120 negative primary tumors.

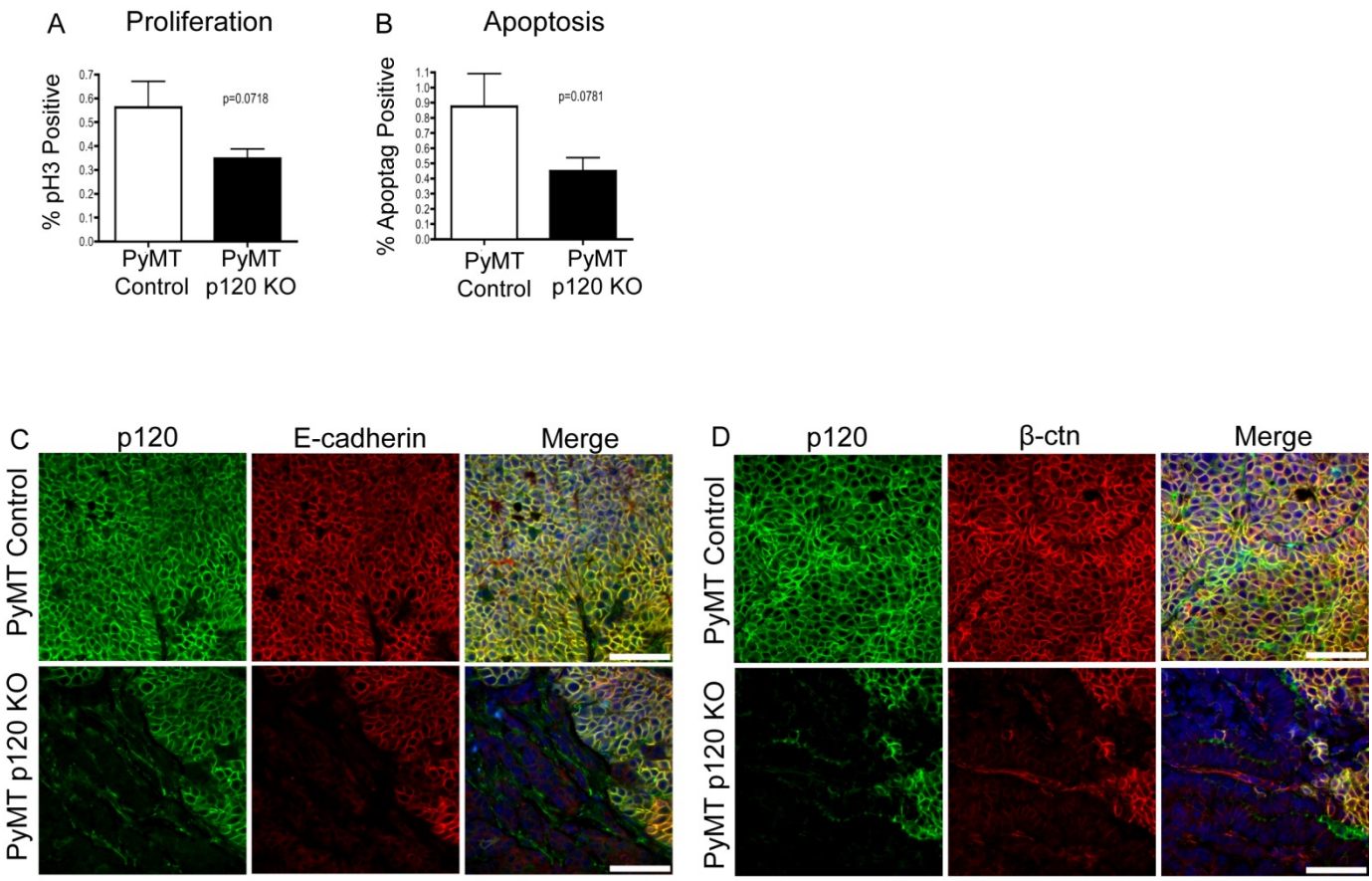


**Supplemental Figure 1**

Figure S1: Further characterization of primary tumors from PyMT p120 KO mice. (A) To assess proliferation, PyMT tumors were stained for phosphorylated histone H3 by immunofluorescence. (B) To assess apoptosis, TUNEL was performed on PyMT tumors. The percent of positive nuclei was assessed in 3 different pseudopapillary regions per n=6 tumors of each genotype. No significant difference in rates of proliferation or apoptosis was observed using Mann-Whitney tests. All scale bars = 50 μM. (C, D) Representative PyMT and PyMT p120 KO tumors were co-immuno- stained for p120 and E-cadherin or p120 and β-catenin. Scale bars = 50 μM.

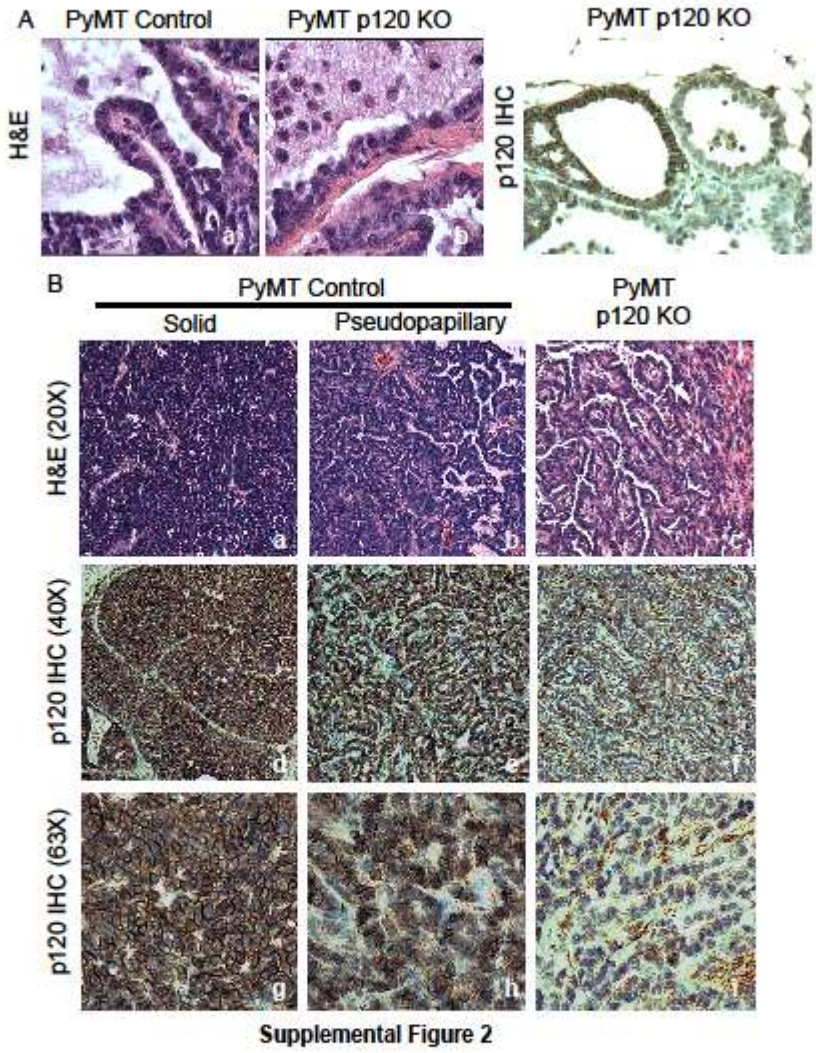


Figure S2: p120 ablation results in cell rounding in hyperplastic ducts and a pseudopapillary phenotype

(A) Early lesions. Sections from control and p120 KO tumors were imaged after hematoxylin and eosin staining or IHC for p120. (B) Late stage lesions. Sections were imaged after hematoxylin and eosin staining or IHC for p120. While control mice exhibited both solid and pseudopapillary regions, p120 loss was solely pseudopapillary.

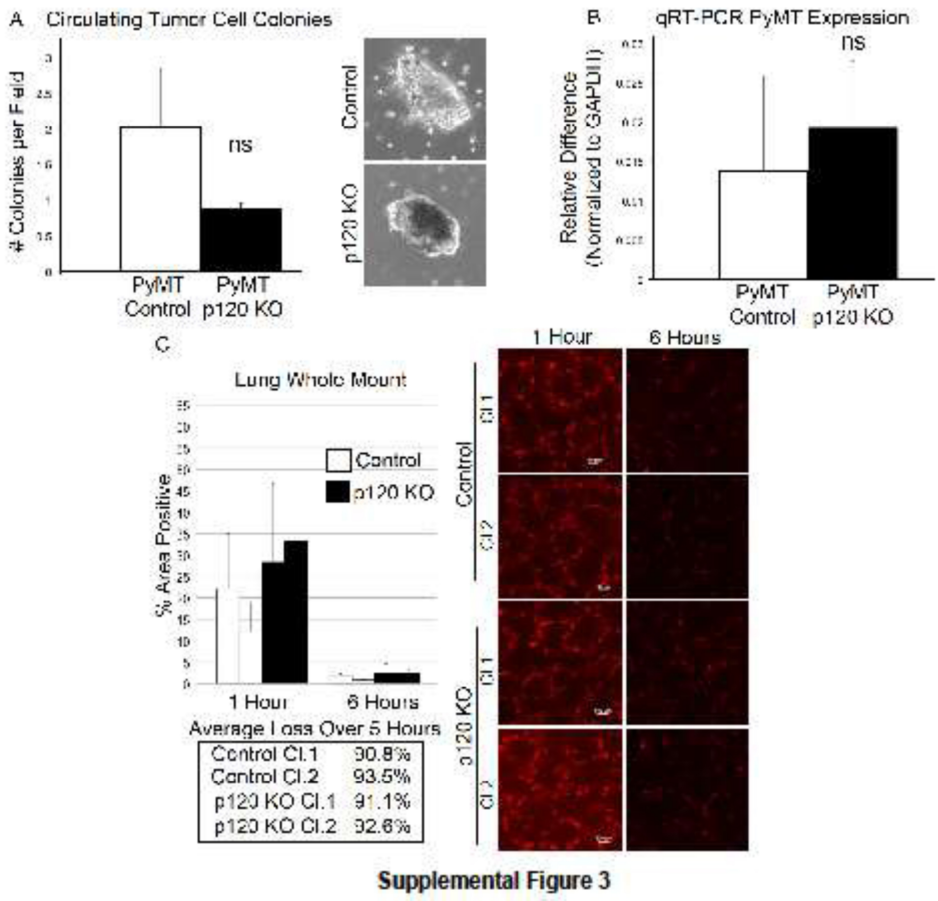


**Supplemental Figure 3**

Figure S3. p120 ablation does not alter circulating tumor cell amounts or luminal survival/ extravasation kinetics

(A) CTC Colony forming assay. Whole blood collected from late stage PyMT mice (n=7 Control and n=5 p120 KO) was plated on matrigel and colony formation from circulating tumor cells was assessed. Graph depicts number of colonies per 2.5x field. Mann-Whitney test ns= no significance. Representative images of colonies are shown. (B) qRT-PCR Analysis of CTC PyMT expression. RNA

from blood of late stage PyMT mice (n=3 per genotype) was assessed for PyMT transcript expression. Data are presented relative to GAPDH control. Mann-Whitney test ns= no significance. (C) Fluorescently labeled PyMT-derived cells were injected into the tail veins of mice (n=3 per cell line and time point) and quantified by lung whole mount after 1 or 6 hours. Data are average with error bars of standard deviation. Percent loss of fluorescent signal from 1 to 6 hours for each clone is stated. Representative images are shown. Scale bars = 100uM.

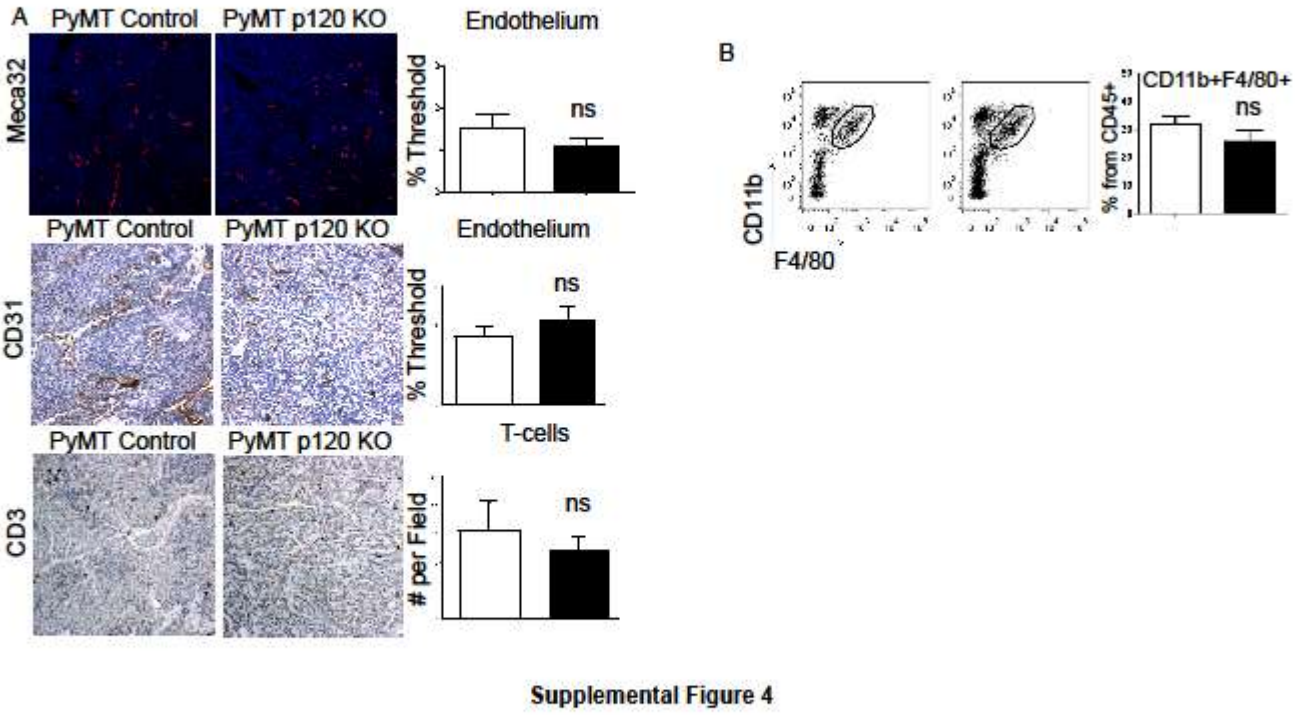


**Supplemental Figure 4**

Figure S4: Unchanged events to the tumor microenvironment after p120 ablation

(A) p120 ablation did not change the following tumor microenvironmental events. PyMT tumors were immuno-stained for Meca-32 to detect endothelial cells. Nuclei are stained with Hoechst dye. IHC for CD31 and CD3 was used to detect endothelial and T-cells, respectively. Mann-Whitney test: ns= no significance. White bars are PyMT Control and black bars are PyMT p120 KO. (B) Representative FACS plots of macrophage numbers in tumor tissue. Plots are gated as CD45+DAPI- .Flow cytometry analysis of CD45+CD11b+F4/80+ cells in tumor tissue.

**Table S1: Patient Cohort Details ( n=1126 )**

| | |
|---|---|
| Age at diagnosis[a] | |
| median (min - max) | 61 (20-98) |
| Tumor diameter (cm) [b] | |
| median (min - max) | 2.2 (0.1-15) |
| Follow-up time (months)[c] | |
| mean (min - max) | 8.5 (1 - 168) |
| median | 52 |
| Tumor grade[d] | |
| G1 | 177 (15.9%) |
| G2 | 524 (46.9%) |
| G3 | 415 (37.2%) |
| Tumor stage[e] | |
| pT1 | 465 (41.5%) |
| pT2 | 489 (43.6%) |
| pT3 | 50 ( 4.5%) |
| pT4 | 117 (10.4%) |
| Axillary nodal status[f] | |
| Node negative (pN0) | 265 (32.8%) |
| Node positive (pN1-3) | 543 (67.2%) |
| ER status[g] | |
| Negative | 212 (19.8%) |
| Positive | 857 (80.2%) |
| E-cadherin status[h] | |
| Negative | 60 ( 5.6%) |
| Positive | 1021 (94.4%) |
| HER2 status[i] | |
| HER2 not amplified | 925 (85.6%) |
| HER2 amplified | 155 (14.4%) |
| Survival[j] | |
| 5 year | 77.3 % |
| 10 year | 60.0 % |

[a] 174 cases missing
[b] 5 cases missing
[c] 191 cases missing
[d] 10 cases missing
[e] 5 cases missing
[f] 318 cases missing
[g] 57 cases missing
[h] 45 cases missing
[i] 46 cases missingi
[j] % given as valid %